

PROCEEDINGS OF THE ROYAL SOCIETY B

BIOLOGICAL SCIENCES

The apparent exponential radiation of Phanerozoic land vertebrates reflects spatial sampling biases

Journal:	<i>Proceedings B</i>
Manuscript ID	RSPB-2020-0372
Article Type:	Research
Date Submitted by the Author:	19-Feb-2020
Complete List of Authors:	Close, Roger; University of Birmingham, School of Geography, Earth and Environmental Sciences Benson, Roger; University of Oxford, Department of Earth Sciences Alroy, J; Macquarie University, Biological Sciences Carrano, Matthew; Smithsonian Institution, Paleobiology; Cleary, Terri; University of Birmingham, School of Geography and Earth Sciences Dunne, Emma; University of Birmingham, School of Geography and Earth Sciences Mannion, Philip; University College London, Earth Sciences; Uhen, Mark; George Mason University, Department of Atmospheric, Oceanic, and Earth Sciences Butler, Richard; University of Birmingham, School of Geography and Earth Sciences
Subject:	Palaeontology < BIOLOGY, Evolution < BIOLOGY, Ecology < BIOLOGY
Keywords:	Species diversity, Macroevolution, Phanerozoic, Sampling standardisation, Tetrapods
Proceedings B category:	Palaeobiology

SCHOLARONE™
Manuscripts

Author-supplied statements

Relevant information will appear here if provided.

Ethics

Does your article include research that required ethical approval or permits?:

This article does not present research with ethical considerations

Statement (if applicable):

CUST_IF_YES_ETHICS :No data available.

Data

It is a condition of publication that data, code and materials supporting your paper are made publicly available. Does your paper present new data?:

Yes

Statement (if applicable):

Data are taken from the Paleobiology Database (www.paleobiodb.org) and can be downloaded from the web interface. We will make the original downloads available via Dryad upon acceptance, but they are too large to be uploaded to Manuscript Central as supplementary material.

Conflict of interest

I/We declare we have no competing interests

Statement (if applicable):

CUST_STATE_CONFLICT :No data available.

Authors' contributions

This paper has multiple authors and our individual contributions were as below

Statement (if applicable):

RJB and RAC conceived the study. JA, MTC, MDU, PDM, RJB, RBB, TJC and EMD contributed to the data set. RAC designed and conducted the analyses, and made the figures. RBB and RJB provided methodological input. RJB and RAC wrote the manuscript. All authors provided critical feedback on the text.

The apparent exponential radiation of Phanerozoic land vertebrates is an artefact of spatial sampling biases

Roger A. Close^{1,*}, Roger B. J. Benson², John Alroy³, Matthew T. Carrano⁴, Terri J. Cleary¹, Emma M. Dunne¹, Philip D. Mannion⁵, Mark D. Uhen⁶, Richard J. Butler^{1,*}

¹School of Geography, Earth and Environmental Sciences, University of Birmingham, Edgbaston, Birmingham B15 2TT, UK.

²Department of Earth Sciences, University of Oxford, Oxford OX1 3AN, UK.

³Department of Biological Sciences, Macquarie University, NSW 2109, Australia.

⁴Department of Paleobiology, National Museum of Natural History, Smithsonian Institution, Washington DC 20013, USA.

⁵Department of Earth Sciences, University College London, London WC1E 6BT, UK.

⁶Department of Atmospheric, Oceanic, and Earth Sciences, George Mason University, Fairfax, VA 22030, USA.

*Authors for correspondence. Email: r.a.close@bham.ac.uk, r.butler.1@bham.ac.uk

Abstract: There is no consensus about how terrestrial biodiversity was assembled through deep time, and in particular whether it has risen exponentially over the Phanerozoic. Using a database of 60,859 fossil occurrences, we show that the spatial extent of the worldwide terrestrial tetrapod fossil record itself expands exponentially through the Phanerozoic. Changes in spatial sampling explain up to 67% of the change in known fossil species counts and, because these changes are decoupled from variation in habitable land area that existed through time, this therefore represents a real and profound sampling bias that cannot be explained as redundancy. To address this bias, we estimate terrestrial tetrapod diversity for palaeogeographic regions of approximately equal size. We find that regional-scale diversity was constrained over timespans of tens to hundreds of millions of years, and similar patterns are recovered for major subgroups, such as dinosaurs, mammals, and squamates. Although Cretaceous/Paleogene mass extinction catalysed an abrupt two- to three-fold increase in regional diversity 66 million years ago, no further increases occurred, and recent levels of regional diversity do not exceed those of the Paleogene. These results parallel those recovered in analyses of local community-level richness. Taken together, our findings strongly contradict past studies that suggested unbounded diversity increases at local and regional scales over the last 100 million years.

Keywords: Biodiversity, Tetrapoda, Phanerozoic, terrestrial, diversification, palaeontology, palaeobiology, macroecology

1. Introduction

Life on land today is spectacularly diverse, accounting for 75–85% of all species [1,2]. Understanding how terrestrial diversity was assembled through deep time is crucial for settling fundamental debates about the diversification process, such as whether it is constrained by ecological limits [3,4]. However, there is no consensus about the long-term

42 trajectory of terrestrial diversity – in particular, whether or not exponential increases through
43 the Phanerozoic have led to diversity being higher today at local, regional, and global scales
44 than at any point in the geological past [3,5-11].

45 Tetrapods today comprise >30,000 extant species and include many of the most iconic and
46 intensely studied groups of animals. Curves of global Phanerozoic tetrapod palaeodiversity
47 have been widely used as exemplars of terrestrial diversification [3,7,9]. In particular, they
48 have been used to argue for an ‘expansionist’ model of diversification, characterised by
49 unconstrained and apparently exponential increases in diversity at a variety of spatial scales,
50 perhaps even driving a tenfold rise in species richness during the last 100 million years [7,8].
51 Within this paradigm, mass extinctions act only as short-term setbacks within a trend of ever-
52 increasing diversity. This expansionist interpretation of terrestrial diversity through deep time
53 has been cited as evidence that contradicts a role for ecological limits in constraining
54 diversification [3], and to propose fundamentally different diversification processes in the
55 marine and terrestrial realms [8].

56 However, the only diversity curves spanning the entire Phanerozoic evolutionary history of
57 tetrapods are based on first and last appearance data for families, drawn from compilations
58 that are now decades old [5,9]. Families are defined inconsistently [12,13], and may not
59 reflect patterns of diversity at the species level. Moreover, these curves do not account for
60 pervasive and long-established spatial and temporal sampling biases [14-16], since they pre-
61 date the widespread use of sampling standardisation methods.

62 Most problematically of all, ‘global’ palaeodiversity curves based on the worldwide fossil
63 record are not truly global, because the spatial extent of the fossil record varies substantially
64 through intervals of geological time [10,11]. In reality, the ‘global’ fossil record comprises a
65 heterogeneous set of regional assemblages, with palaeogeographic regions that vary markedly
66 in number, identity, and extent (both within and between continental regions) through
67 intervals of geological time. Critically, the palaeogeographic spread (=spatial extent) of the
68 terrestrial fossil record itself grows exponentially through the Phanerozoic (Figs 1B and Fig.
69 2; see also Figs S1 and S2), and is decoupled from the actual terrestrial area that existed
70 through time (see Results). Such changes in the geographic extent of the sampled fossil
71 record will substantially bias patterns of diversity through time, even when using sampling-
72 standardised richness estimators [17].

73 Patterns inconsistent with expansionism are recovered by analyses applying rigorous
74 sampling standardisation to estimate regional diversity of more restricted groups of tetrapods
75 [6,18-20], or over shorter intervals of time (the Mesozoic–early Paleogene; [10,11]).
76 Analyses of Phanerozoic tetrapod diversity at the local-community scale [21] also contradict
77 the expansionist model of diversification. However, it remains unclear how terrestrial
78 tetrapod diversity at regional spatial scales changed through the entirety of the Phanerozoic,
79 especially from the Paleogene to the present, when the most substantial increases in face-
80 value ‘global’ curves are observed.

81 Here, we present the first regional-scale diversity patterns for terrestrial tetrapods that cover
82 their entire Phanerozoic evolutionary history, while adequately correcting for key biases. In
83 doing so, we interpret the structure of the fossil record as an array of well-sampled
84 palaeogeographic regions that contain useful information about regional palaeodiversity, but
85 which are only indirectly informative about true global palaeodiversity. To achieve this, we
86 extend and substantially improve our recently-developed approach for addressing large-scale
87 spatial sampling biases [11]. We conduct our analyses at the species level, and compare our
88 results to different models the diversification process. Our results demonstrate that diversity
89 curves based on face-value counts of taxa from the ‘global’ fossil record primarily reflect

90 major increases in the geographic spread of fossil localities towards the present day. After
91 controlling for these biases, we find no evidence for expansionist diversification in regional
92 assemblages. The similarity of this regional pattern to patterns of local richness [21] suggests
93 that beta diversity is unlikely to have changed substantially over the Phanerozoic, although
94 further work is needed to confirm this. These results imply that the global diversity present in
95 terrestrial ecosystems today may be similar to that of the early Cenozoic.

96

97 **2. Methods**

98 *Overview of analytical procedure.* We estimated diversity and other variables for
99 palaeogeographic regions with approximately equal sizes. To achieve this, our analysis
100 implemented the following steps (each described in more detail below):

- 101 1. We downloaded occurrence data for Phanerozoic non-flying tetrapods and key
102 subgroups from the Paleobiology Database (Fig. 3A; Figs S1), removed unsuitable
103 records, and binned the remaining records within equal-length time intervals.
- 104 2. We used a spatial subsampling algorithm (described below) to identify all nested
105 subsets of adjacent fossil localities (=subsampled palaeogeographic regions) for each
106 time interval, using the set of palaeocoordinates for all collections yielding non-flying
107 terrestrial tetrapods (Fig. 3C).
- 108 3. We computed variables of interest (diversity, spatial metrics, etc.) for each
109 subsampled palaeogeographic region.
- 110 4. We standardised the spatial extent of sampling in the fossil record by identifying
111 subsampled palaeogeographic regions that simultaneously met a set of criteria related
112 to spatial extent (summed MST length) and other spatial and sampling-related metrics
113 (see below). This was performed at several distinct spatial scales.
- 114 5. We identified clusters of overlapping palaeogeographic regions (Fig. 3D; see below).
115 This is necessary because palaeogeographic regions identified via the exhaustive
116 search algorithm implemented in Step 2 may share many of the same underlying
117 fossil localities.
- 118 6. All variables computed for palaeogeographic regions were summarised for each
119 spatial cluster by computing medians and interquartile ranges.

120 *Dataset.* We downloaded fossil occurrence data for Phanerozoic Tetrapodomorpha from the
121 Paleobiology Database [22] on 27 February 2019. We also downloaded occurrences for key
122 tetrapod subgroups (Dinosauromorpha, Probainognathia, Squamata, Pseudosuchia,
123 Testudinata, and Lissamphibia), and used the ‘occurrence_no’ fields from these downloads to
124 filter records from the main occurrence dataset. All occurrence datasets were downloaded
125 using the Paleobiology Database API [23], using function calls executed within the analysis
126 R scripts (URLs used to perform these data downloads, together with all analysis scripts, are
127 available on Dryad [XXX]).

128 We removed unsuitable records from the occurrence dataset largely following the procedures
129 outlined in Close et al. [11]. Contrary to that study, however, we did not exclude collections
130 from deposits that were unlithified or partially-lithified and sieved (this is because
131 lithification biases more severely affect the face-value estimates of local richness analysed
132 Close et al. [11]). The patterns we document here are therefore conservative with respect to
133 lithification biases, which manifest primarily from the Late Cretaceous onwards and become
134 more profound towards the present. Flying tetrapods (Aves, Pterosauromorpha, and
135 Chiroptera) were excluded because their fossil record is inadequate in most intervals and
136 regions, and Lagerstätten-dominated. After cleaning, the dataset comprised 17,323

137 collections (broadly equivalent to fossil localities; see discussion in [21] for more detail),
138 yielding 60,859 occurrences of 14,023 non-flying, non-marine tetrapod species.

139 Following previous studies (e.g. [11]), we used composite time bins of approximately equal
140 length (~10 myr; Table S1). Occurrences were assigned to a bin if that bin contained over
141 50% of the geologic time range associated with that occurrence (defined by the early and late
142 bounds recorded by the 'min_ma' and 'max_ma' fields in the Paleobiology Database, in Ma).
143 A total of 4,056 occurrences were dropped because they did not meet these binning criteria
144 (72,413 before and 68,357 after).

145 *Identifying subsampled palaeogeographic regions.* To control for the pervasive spatial
146 sampling biases affecting the terrestrial fossil record, we estimated diversity and other key
147 variables for approximately equally-sized palaeogeographic regions, which we defined by
148 drawing spatial subsamples of adjacent fossil localities (on a per-interval basis). To define
149 these palaeogeographic regions, we used a spatial subsampling algorithm that identifies all
150 nested sets of adjacent spatial points [24]. Spatial points were defined by binning the
151 palaeocoordinates for all collections in our cleaned occurrence dataset into equal-size
152 hexagonal/pentagonal grid cells with 100 km spacings (Fig. 3A–B), using the R package
153 dggridR [25]. Spatial points used in our spatial subsampling algorithm are therefore 100 km
154 grid cells containing at least one fossil occurrence.

155 The spatial subsampling algorithm works by: 1) selecting a random spatial point as a starting
156 location; 2) identifying the closest spatial point, choosing at random if there are two or more
157 equidistant points; 3) saving these two points as a palaeogeographic region; 4) identifying the
158 closest point to those two points; 5) saving this set as a palaeogeographic region, and 6)
159 continuing this procedure until all spatial points have been added. The algorithm is then
160 repeated for every possible starting location, and any duplicate palaeogeographic regions are
161 discarded. Distances were calculated from midpoints of 100 km dggridR cells. This
162 procedure results in a database of palaeogeographic regions (sets of directly-adjacent or
163 nearest-neighbour fossil localities) covering all possible sizes (Fig. 3C).

164 Palaeogeographic regions were identified using the set of fossil localities for the most
165 inclusive taxon set that we analysed (i.e. non-flying, non-marine tetrapods). Diversity
166 estimates for individual tetrapod subclades were also derived from these same
167 palaeogeographic regions, because these represent areas in which tetrapod subclades could
168 potentially be sampled.

169 Each palaeogeographic region was then characterised by computing a wide range of different
170 metadata (e.g. variables relating to diversity, spatial factors, or sampling metrics). Spatially-
171 standardised sets of palaeogeographic regions were obtained by simultaneously applying sets
172 of filtering criteria (e.g. relating to spatial extent, numbers of occupied grid cells, etc.; see
173 below).

174 *Variables calculated for subsampled palaeogeographic regions.* We calculated a wide variety
175 of metadata for each palaeogeographic region. Spatial variables include counts of occupied
176 equal-area grid cells (i.e. cells yielding fossil occurrences) spanning a range of sizes (100,
177 200, 500, 1,000 and 5,000 km spacings, calculated using the R package dggridR [25]); our
178 primary measure of palaeogeographic spread, minimum-spanning tree (MST) length (= the
179 minimum total length of all the segments connecting spatial points in a region [26]; see Close
180 et al. [11] for justification); the distance of the longest branch in each MST (used to identify
181 spatial regions with widely-separated clusters of localities). Sampling variables include
182 counts of literature references reporting the fossil occurrences in each spatial region (used as

183 a proxy for research effort) and measures of sample coverage (Good's u [27] and the multiton
184 ratio [28]).

185 We estimated species richness within palaeogeographic regions using four very different
186 methods: face-value counts of species within regions (= raw or uncorrected richness; i.e. not
187 sampling standardised), Shareholder Quorum Subsampling (SQS [26,29,30], also known as
188 coverage-based rarefaction [31]); and the asymptotic extrapolators 'squares' [32] and Chao 2
189 [33].

190 We focus primarily on patterns estimated using SQS, which provides an objective,
191 frequency-dependent measure of diversity that is insensitive to variation in sampling [31].
192 Standardising to equal sample coverage may increase the signal of evenness at lower quorum
193 levels [17]. Nonparametric asymptotic richness extrapolators, on the other hand, are less
194 sensitive to evenness, but are downward biased when sample sizes are insufficient for
195 estimates to have asymptoted [17]. We therefore present estimates using both approaches.
196 Face-value counts of species within palaeogeographic regions, meanwhile, facilitate direct
197 comparison with existing face-value 'global' curves.

198 We implemented SQS using the analytical solutions in the R package iNEXT [34]), which
199 allows seamless integration of interpolated (=subsampled), observed and extrapolated
200 coverage-standardised species richness estimates. We used quorum levels of 0.4, 0.6 and 0.8.

201 *Grid-cell rarefaction algorithm.* To additionally control for variation in the 'packing density'
202 or spatial coverage of fossil localities within equal-sized palaeogeographic regions, we used a
203 grid-cell rarefaction (GCR) procedure prior to calculating our focal measure of diversity,
204 SQS (other estimators were not subject to this procedure due to heavy computational
205 demands). When using GCR, SQS was estimated for each palaeogeographic region at a range
206 of subsampled grid-cell quotas (we present GCR results using quotas of 3, 5 and 8 occupied
207 200 km equal-area grid-cells with per 1,000 km of MST length, calculated using 50
208 subsampling trials). SQS richness was also estimated without GCR (GCR = 'off'). To
209 compare different richness estimators on an equal footing, our focal results do not use SQS
210 with grid-cell rarefaction.

211 *Standardising spatial sampling.* To standardise spatial sampling, we identified subsampled
212 palaeogeographic regions that simultaneously met the following criteria:

- 213 1. Seven distinct spatial scales, comprising minimum-spanning tree (MST) lengths of
214 1,000 km, 1,500 km, 2,000 km, 2,500 km, 3,000 km, 3,500 km and 4,000 km ($\pm 10\%$;
215 Fig. 3C and S3). We quantified palaeogeographic spread using MSTs for reasons
216 outlined by Close et al. [11]);
- 217 2. MSTs for which the length of the longest branch was no more than 40% of the total
218 MST size (in order to exclude clusters of localities separated by large gaps);
- 219 3. At least 20 literature references, to ensure a minimum level of study;
- 220 4. A multiton ratio [28] of at least 0.25, to exclude palaeogeographic regions with very
221 poor sample completeness (sometimes estimates of Good's u may spuriously appear
222 high for small sample sizes, and the multiton ratio offers a more conservative and
223 partially-independent measure of sample completeness).

224 We also excluded palaeogeographic regions that crossed geographic barriers, based on the
225 combined presence of countries or continental regions at particular points in time (South
226 America and Africa after 120 Ma; Australia and New Zealand after 70 Ma; Europe and
227 Africa after 66 Ma).

228 *Spatial clustering algorithm.* Because our spatial subsampling algorithm finds all nested sets
 229 of adjacent spatial points, the full set of palaeogeographic regions will invariably include
 230 some regions that share underlying spatial points to a greater or lesser degree (ranging from
 231 no overlap to almost complete overlap). To address potential issues with non-independence
 232 between data points inflating apparent sample size, we identified clusters of similar
 233 palaeogeographic regions based on the fraction of spatial points they shared (samples were
 234 added to a spatial cluster if they shared >25% of the spatial points with another sample in the
 235 cluster; Figs 3D and S4). Key variables such as diversity and spatial or sampling metrics
 236 were then summarised for each cluster of palaeogeographic regions by computing median
 237 values and interquartile ranges.

238 *Model Comparisons.* We used linear model comparisons to examine whether patterns of
 239 spatially-standardised diversity are more consistent with diversification that is unconstrained
 240 ('expansionist', with steady increases through time) or constrained (i.e. with long-lived
 241 diversity equilibria, separated by phase-shifts). Our linear models included combinations of
 242 three explanatory variables: (1) absolute time, representing continuous per-lineage
 243 diversification; (2) an intercept, representing a null model in which diversity is static through
 244 time; and (3) a diversification-phase variable in which the intercept and/or slope are allowed
 245 to differ before and after the Cretaceous/Paleogene (K/Pg) mass extinction (66 Ma). Phase
 246 was included both as a covariate (allowing the intercept to vary independently between
 247 phases) and an interaction term (allowing the intercept and slope to vary between phases; see
 248 Table 1 for full list of models). These models were compared against an intercept-only null
 249 model. Richness estimates were log-transformed. Models were ranked using Akaike
 250 Information Criteria with the adjustment for small sample sizes (AICc) [35].

251 *Interactive data explorer.* Patterns of spatially-standardised diversity and other variables can
 252 be explored interactively using a Shiny web application, available as a gist on GitHub. The
 253 application can be run within RStudio by executing the following command:

254 `shiny::runGist('https://gist.github.com/rclose/URL-to-come-after-acceptance')`

255 **[Note to reviewers: to make access to the interactive Shiny application easier during peer-**
 256 **review, we have make it available as an online web application accessible at**
 257 **<https://factsaboutgiraffes.shinyapps.io/test-plot/>. The free tier for shinyapps.io permits 25**
 258 **hours of use per month, which should suffice for review purposes. However, it would**
 259 **probably not be enough for post-publication usage, so we will use the Gist described above**
 260 **instead.]**

261 The interactive data explorer allows exploration of spatially-standardised diversity results for
 262 all taxon sets, richness and other variables. Clicking on a data point plots the underlying data
 263 on a palaeomap and displays tables of the underlying occurrence data in that
 264 palaeogeographic region.

265 3. Results

266 The palaeogeographic spread (=spatial extent) of the terrestrial fossil record grows
 267 exponentially through the Phanerozoic (Figs 1B and Fig. 2; see also Figs S1 and S2), and is
 268 decoupled from the actual terrestrial area that existed through time. Although the
 269 palaeogeographic spread of the sampled fossil record increases fourfold through the
 270 Cenozoic, increases in actual terrestrial area over the same interval are much smaller (~15%;
 271 [36]; Fig. 1B; Fig. S5). Changes (i.e., first differences) in the palaeogeographic extent of the
 272 'global' fossil record of terrestrial tetrapods explain approximately 24–67% of changes in
 273 face-value species counts, and 31–34% of the changes in subsampled richness estimates,

274 depending on the measure of palaeogeographic spread used (Figs 1C–D and S6). By contrast,
275 changes in the palaeogeographic spread of the fossil record are not significantly correlated
276 with changes in continental area (Figs 1E–F and S7). The strong correlations observed
277 between diversity and spatial sampling therefore represent real and profound sampling biases
278 [10,11,17,21] that cannot be explained by ‘redundancy’ or ‘common cause’ effects [37,38].

279 The non-marine sedimentary rock record also decays exponentially with increasing age due
280 to the progressive loss of sediments to erosion and burial, and is therefore likely to exert
281 some influence on the palaeogeographic spread of fossil localities through time [16,39,40].
282 Surprisingly, though, we find that neither changes in ‘global’ diversity nor the
283 palaeogeographic spread of the fossil record are significantly correlated with changes in
284 extent of non-marine sediments (Fig. S8). This indicates that the rock record is not the
285 primary factor controlling spatial sampling in the terrestrial fossil record, and further justifies
286 our direct use of the palaeogeographic distribution of the tetrapod fossil record to estimate
287 spatially-standardised diversity patterns. Generalised least-squares models (GLS) of ‘global’
288 diversity, as a function of the palaeogeographic spread of the worldwide fossil record,
289 continental area and non-marine sediment extent (modelling temporal autocorrelation using a
290 first-order autoregressive structure), recover a strong, statistically significant explanatory role
291 only for palaeogeographic spread (Table 2).

292 Because pervasive spatial bias prevents us from estimating meaningful time series of global
293 diversity through the Phanerozoic, we recommend that studies must instead focus on
294 estimating regional-scale diversity for well-sampled palaeogeographic regions. The patterns
295 of spatially-standardised regional richness that we recover are broadly consistent across
296 spatial scales and for different richness estimators (Fig. 4). Surprisingly, results are highly
297 congruent even when using face-value counts of species from spatially-standardised regions
298 (in other words, when spatial sampling is standardised, but sampling intensity is not; Fig. 4).
299 This suggests that variation in the spatial scope of the terrestrial fossil record has a more
300 pronounced effect on apparent species richness than does variation in intensity or
301 completeness of sampling within those regions.

302 Although data are insufficient to estimate regional diversity for much of the Paleozoic, levels
303 during the latest Permian (~255 Ma) appear to have been similar to those of the Early
304 Triassic (~250 Ma; Fig. 4). Similar regional diversity estimates are maintained up until the
305 latest Cretaceous (~70 Ma), spanning a total interval exceeding 180 million years. Linear
306 regressions of diversity on time for this extended interval return non-significant slopes,
307 indicating a long-term static pattern of standing regional diversity (Fig. S9). This is true
308 despite substantial faunal turnover throughout, including the Permian/Triassic (P/T) mass
309 extinction (252 Ma), and the initial origins of groups that are speciose today during the
310 Jurassic and Cretaceous [41].

311 Nevertheless, there are two clear intervals when regional-scale tetrapod diversity apparently
312 increased substantially. All tetrapods share a single ancestor species that lived no later than
313 the Late Devonian [42]. Although the data are insufficient to obtain diversity estimates
314 during the Carboniferous, early increases in terrestrial tetrapod diversity must therefore have
315 occurred within the Carboniferous to mid-Permian. A large apparent increase in maximum
316 regional diversity also occurred later, in the aftermath of the K/Pg mass extinction [10,11,21].
317 This primarily results from the fossil record of mammals, which shows an abrupt three- to
318 fourfold increase in regional diversity (Fig. 5). There is no evidence in our data for
319 substantial increases in maximum regional diversity through the remainder of the Cenozoic,
320 either in tetrapods as a whole, or in major subclades (Figs 4 and 5). In fact, linear regressions
321 of regional diversity on time for the Cenozoic recover significant trends towards lower

322 richness through time, driven by lower diversity in bins Ng3 and Ng4 (approximately the last
323 10 million years; Fig. S9).

324 Model selection using information criteria demonstrates that the best explanations of regional
325 diversity include the passage of time and a phase-shift across the K/Pg boundary. Across all
326 spatial standardisation criteria, the model including time and phase as an interaction term
327 receives greatest support (Table 1). This is because there is a shift to a higher regional
328 diversity equilibrium across the K/Pg boundary, but this is followed by a significant decrease
329 in regional diversity towards the present (Table S2; Fig. S9). For other richness estimators,
330 see Supplementary Results.

331 Grid-cell rarefaction results highlight that the density of spatial coverage inside standardised
332 palaeogeographic regions increases towards the present: when higher quotas of occupied grid
333 cells are imposed, many more data points are excluded from the Paleozoic–Mesozoic than
334 from the Cenozoic (Fig. S10).

335

336 **4. Discussion**

337 Although long under-appreciated, variable spatial sampling represents a fundamental fossil
338 record bias, and one that must be accounted for. Our results show that previous
339 interpretations of exponential increases in tetrapod diversity through the Phanerozoic are an
340 artefact of the increasing spatial extent of the ‘global’ fossil record (Fig. 1A–B). Between one
341 and two thirds of the changes through time seen in ‘global’ diversity curves can be explained
342 by changes in the palaeogeographic extent of sampled fossil localities (Figs 1B, D and S6),
343 and this covariation is not explained by changes in the actual amount of habitable land area
344 (Fig. S7E–H) or the extent of non-marine sediments (Fig. S8F–J). Although changes in
345 continental area and the extent of non-marine sediments through time likely do exert some
346 influence on the worldwide palaeogeographic spread of the terrestrial fossil record
347 (particularly the extent of non-marine sediments, which decreases exponentially with
348 increasing age [40]), other factors appear to be at least as important.

349 Estimating truly representative ‘global’ diversity curves for terrestrial tetrapods is, therefore,
350 almost certainly not possible based on our current knowledge of the fossil record, and
351 diversity analyses must focus on local and regional scales. We present the first spatially-
352 standardised regional richness estimates spanning the entire evolutionary history of tetrapods.
353 By estimating diversity for comparably-sized palaeogeographic regions through time, we
354 recover fundamentally different patterns of diversity change to those found by previous
355 studies of face-value ‘global’ trends [5,9], even when we consider only face-value species
356 counts that do not control for variation in sampling intensity (Fig. 4). Most notably, variation
357 in regional diversity within individual time bins is usually on par with variation through time,
358 leading to patterns that are constrained over timescales of up to ~180 million years. We find
359 no support for large sustained increases over the last 100 million years.

360 We do, however, observe an abrupt increase in regional-scale terrestrial tetrapod diversity
361 during the earliest Cenozoic, consistent with recent work at local to continental spatial scales
362 [10,11,21]. The precise reasons for this step-change are currently uncertain. It may support a
363 fundamental role for the K/Pg mass extinction in disrupting and reorganising terrestrial
364 ecosystems, consistent with a role for ecological limits in regulating diversification [4].
365 Mammals certainly experienced a large increase in richness in the early Cenozoic. However,
366 the relative contribution of mammals to overall tetrapod diversity patterns – and thus the
367 magnitude of the increase itself – is likely exaggerated, due to their high preservation
368 potential and the ease of diagnosing species from isolated teeth: in the Cenozoic fossil record,

369 mammal diversity is more than twice that of squamates (Fig. 5), yet the reverse is true for
370 extant species richness. In contrast, the P/T extinction, the largest in Earth history, does not at
371 present appear to have played a similar role in elevating long-term diversity (although sparse
372 Paleozoic data limits interpretations). The reasons for the differing long-term impacts of the
373 P/T and K/Pg extinctions on standing terrestrial diversity are unclear, but may reflect
374 differences in the timescales over which the two events took place, or variation in the biology
375 and preservation potential of the groups that flourished in the aftermath of each event.

376 Meanwhile, we find no evidence for effects on regional diversity of other events in
377 evolutionary history of terrestrial tetrapods that have been hypothesised to have catalysed
378 diversity increases, including the initial expansion of angiosperms during the middle and Late
379 Cretaceous [7], and the breakup of the supercontinent Pangea [43]. This does not rule out a
380 role for events in plant evolution as drivers of tetrapod diversification. Instead, it is possible
381 that floral state-changes across the K/Pg boundary (e.g. increases in seed sizes [44]) might
382 have been more important for mammalian species richness than events within the Cretaceous
383 itself, a hypothesis that requires further investigation. Neither do our analyses of regional
384 diversity rule out some increase in global richness due to continental fragmentation (although
385 we have shown that global diversity cannot currently be estimated). Modelling of species-
386 area relationships suggests that this effect could have approximately doubled global terrestrial
387 tetrapod biodiversity between the Triassic and Late Cretaceous, during the main interval of
388 Pangean fragmentation [43]. Pangean fragmentation was largely complete by the end of the
389 Cretaceous, and it seems unlikely that the comparatively minor continental rearrangements
390 that occurred during the Cenozoic could have driven the proposed ten-fold increase in global
391 diversity recovered by influential previous work [5,9].

392 Our results are consistent with a growing body of evidence from the fossil record for
393 constrained diversification within the terrestrial realm [6,10,11,18,21,32,45,46]. Moreover,
394 the regional-scale patterns we document for Phanerozoic tetrapods are highly congruent with
395 those observed at smaller spatial scales, such as for local richness [21], which also show
396 minimal increases from the late Paleozoic–Mesozoic, a step-change across the K/Pg
397 boundary, and no increase through the Cenozoic. The similarity between patterns of diversity
398 at local (alpha) and regional (gamma) scales suggests an absence of systematic long-term
399 trends in tetrapod beta diversity within regions through the Phanerozoic, although studies of
400 the long-term patterns of beta diversity are needed to confirm this. Although limitations of
401 the fossil record prohibit us from analysing regional-scale flying tetrapod diversity here,
402 within-community patterns suggest these groups (birds, bats, pterosaurs) were also subject to
403 long-term constraints [21]. These patterns suggest that the early diversification of birds
404 resulted in the stepwise addition of substantial species richness to terrestrial ecosystems [10],
405 with limited subsequent increases [21] that mirror the patterns of tetrapod richness
406 documented here.

407 The diversity patterns we present are for regional spatial scales, and thus not directly
408 comparable with global patterns. Furthermore, our results suggest that truly global estimates
409 of tetrapod diversity through geological time are inaccessible based on our current knowledge
410 of the fossil record. Nevertheless, barring substantial and as-yet-unquantified increases in
411 global-scale faunal provinciality (i.e. between continental regions), previous findings of
412 sustained, expansionist increases in ‘global’ standing diversity over the last 100 million years
413 [5,7,9] are most likely artefactual, resulting from a failure to account for exponential
414 increases in the spatial extent of terrestrial sampling over the same interval. Our results
415 provide further evidence to overturn the previous paradigm of unconstrained, expansionist
416 diversification, instead indicating long periods of relative stasis, disrupted by rare,
417 geologically-rapid rises in maximum standing diversity.

418

419 **Acknowledgments:** We thank all contributors to the Paleobiology Database. This is
420 Paleobiology Database official publication XXX. We thank Mike Benton and two
421 anonymous reviewers for helpful review comments.

422 **Funding:** This research was funded by the European Union's Horizon 2020 research and
423 innovation program under grant agreement 637483 (ERC Starting Grant TERRA to RJB).
424 PDM was supported by a Royal Society University Research Fellowship (UF160216).

425 **Author contributions:** RJB and RAC conceived the study. JA, MTC, MDU, PDM, RJB,
426 RBB, TJC and EMD contributed to the data set. RAC designed and conducted the analyses,
427 and made the figures. RBB and RJB provided methodological input. RJB and RAC wrote
428 the manuscript. All authors provided critical feedback on the text.

429

430 **References:**

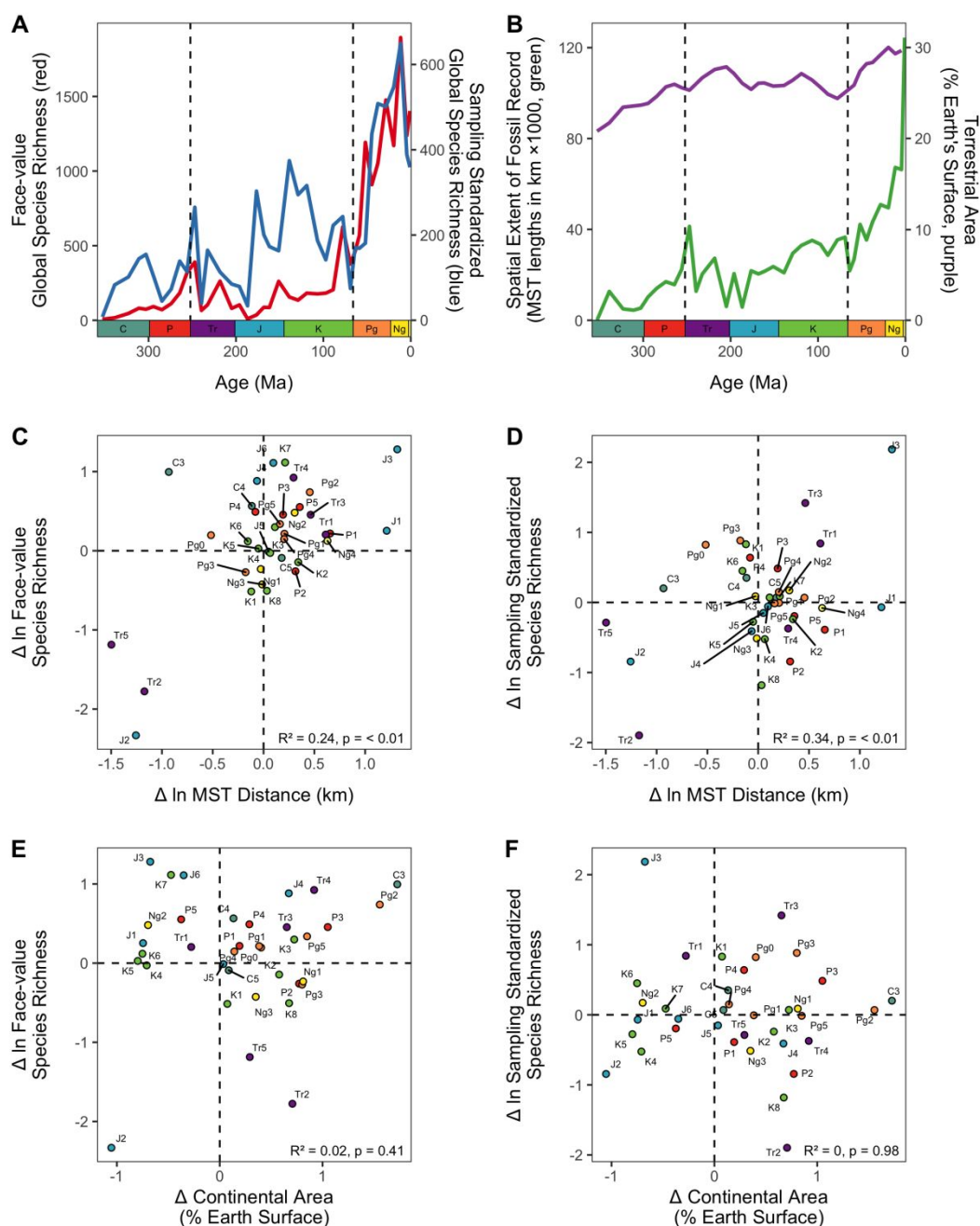
- 431 1. May, R. M. 1994 Biological diversity: differences between land and sea. *Phil. Trans.*
432 *R. Soc. B* **343**, 105–111.
- 433 2. Mora, C., Tittensor, D. P., Adl, S., Simpson, A. G. B. & Worm, B. 2011 How Many
434 Species Are There on Earth and in the Ocean? *PLoS Biol.* **9**, e1001127.
435 (doi:10.1371/journal.pbio.1001127)
- 436 3. Harmon, L. J. & Harrison, S. 2015 Species diversity is dynamic and unbounded at
437 local and continental scales. *Am. Nat.* **185**, 584–593. (doi:10.1086/680859)
- 438 4. Rabosky, D. L. & Hurlbert, A. H. 2015 Species richness at continental scales is
439 dominated by ecological limits. *Am. Nat.* **185**, 572–583. (doi:10.1086/680850)
- 440 5. Benton, M. J. 1996 Testing the roles of competition and expansion in tetrapod
441 evolution. *Proc. R. Soc. B* **263**, 641–646. (doi:10.1098/rspb.1996.0096)
- 442 6. Alroy, J. 2009 Speciation and extinction in the fossil record of North American
443 mammals. In *Speciation and Patterns of Diversity* (eds R. Butlin J. Bridle & D.
444 Schluter), pp. 301–323. Cambridge: Cambridge University Press.
445 (doi:10.1017/CBO9780511815683.017)
- 446 7. Benton, M. J. 2010 The origins of modern biodiversity on land. *Phil. Trans. R. Soc. B*
447 **365**, 3667–3679. (doi:10.1098/rstb.2010.0269)
- 448 8. Vermeij, G. J. & Grosberg, R. K. 2010 The great divergence: when did diversity on
449 land exceed that in the sea? *Integr. Comp. Biol.* **50**, 675–682. (doi:10.1093/icb/icq078)
- 450 9. Sahney, S., Benton, M. J. & Ferry, P. A. 2010 Links between global taxonomic
451 diversity, ecological diversity and the expansion of vertebrates on land. *Biol. Lett.* **6**,
452 544–547. (doi:10.1098/rsbl.2009.1024)
- 453 10. Benson, R. B. J., Butler, R. J., Alroy, J., Mannion, P. D., Carrano, M. T. & Lloyd, G.
454 T. 2016 Near-stasis in the long-term diversification of Mesozoic tetrapods. *PLoS Biol.*
455 **14**, e1002359. (doi:10.1371/journal.pbio.1002359)

- 456 11. Close, R. A., Benson, R. B. J., Upchurch, P. & Butler, R. J. 2017 Controlling for the
457 species-area effect supports constrained long-term Mesozoic terrestrial vertebrate
458 diversification. *Nat. Commun.* **8**, 15381. (doi:10.1038/ncomms15381)
- 459 12. Forey, P. L., Fortey, R. A., Kenrick, P. & Smith, A. B. 2004 Taxonomy and fossils: a
460 critical appraisal. *Phil. Trans. R. Soc. B* **359**, 639–653. (doi:10.1098/rstb.2003.1453)
- 461 13. Stadler, T., Rabosky, D. L., Ricklefs, R. E. & Bokma, F. 2014 On Age and Species
462 Richness of Higher Taxa. *Am. Nat.* **184**, 447–455. (doi:10.1086/677676)
- 463 14. Raup, D. M. 1972 Taxonomic Diversity during the Phanerozoic. *Science* **177**, 1065–
464 1071. (doi:10.1126/science.177.4054.1065)
- 465 15. Smith, A. B. & McGowan, A. J. 2007 The shape of the Phanerozoic marine
466 palaeodiversity curve: how much can be predicted from the sedimentary rock record of
467 western Europe? *Palaeontology* **50**, 765–774. (doi:10.1111/j.1475-4983.2007.00693.x)
- 468 16. Alroy, J. 1998 Equilibrial diversity dynamics in North American mammals. In
469 *Biodiversity Dynamics* (eds M. L. McKinney & J. A. Drake), New York: Columbia
470 University Press.
- 471 17. Close, R. A., Evers, S. W., Alroy, J. & Butler, R. J. 2018 How should we estimate
472 diversity in the fossil record? Testing richness estimators using sampling-standardised
473 discovery curves. *Methods in Ecology and Evolution* **28**, 1023–15. (doi:10.1111/2041-
474 210X.12987)
- 475 18. Cantalapiedra, J. L., Domingo, M. S. & Domingo, L. 2018 Multi-scale interplays of
476 biotic and abiotic drivers shape mammalian sub-continental diversity over millions of
477 years. *Sci Rep* **8**, 1–8. (doi:10.1038/s41598-018-31699-6)
- 478 19. Carrasco, M. A., Barnosky, A. D. & Graham, R. W. 2009 Quantifying the Extent of
479 North American Mammal Extinction Relative to the Pre-Anthropogenic Baseline.
480 *PLoS ONE* **4**, e8331. (doi:10.1371/journal.pone.0008331)
- 481 20. Barnosky, A. D., Carrasco, M. A. & Davis, E. B. 2005 The Impact of the Species–
482 Area Relationship on Estimates of Paleodiversity. *PLoS Biol.* **3**, e266.
483 (doi:10.1371/journal.pbio.0030266)
- 484 21. Close, R. A. et al. 2019 Diversity dynamics of Phanerozoic terrestrial tetrapods at the
485 local-community scale. *Nat. Ecol. Evol.* **3**, 590–597. (doi:10.1038/s41559-019-0811-8)
- 486 22. In press. The Paleobiology Database.
- 487 23. Peters, S. E. & McClennen, M. 2015 The Paleobiology Database application
488 programming interface. *Paleobiology*, 1–7. (doi:10.1017/pab.2015.39)
- 489 24. Lagomarcino, A. J. & Miller, A. I. 2012 The Relationship between Genus Richness
490 and Geographic Area in Late Cretaceous Marine Biotas: Epicontinental Sea versus
491 Open-Ocean-Facing Settings. *PLoS ONE* **7**, e40472.
492 (doi:10.1371/journal.pone.0040472)
- 493 25. Barnes, R. In press. dggridR: Discrete Global Grids for R. R package version 0.1.12.

- 494 26. Alroy, J. 2010 Geographical, environmental and intrinsic biotic controls on
495 Phanerozoic marine diversification. *Palaeontology* **53**, 1211–1235.
496 (doi:10.1111/j.1475-4983.2010.01011.x)
- 497 27. Good, I. J. 1953 The population frequencies of species and the estimation of
498 population parameters. *Biometrika* **40**, 237–264. (doi:10.1093/biomet/40.3-4.237)
- 499 28. Alroy, J. 2017 Effects of habitat disturbance on tropical forest biodiversity. *PNAS* **16**,
500 201611855–16. (doi:10.1073/pnas.1611855114)
- 501 29. Alroy, J. 2010 The shifting balance of diversity among major marine animal groups.
502 *Science* **329**, 1191–1194. (doi:10.1126/science.1189910)
- 503 30. Alroy, J. 2010 Fair sampling of taxonomic richness and unbiased estimation of
504 origination and extinction rates. In *Quantitative methods in paleobiology* (eds J. Alroy
505 & G. Hunt), pp. 55–80.
- 506 31. Chao, A. & Jost, L. 2012 Coverage-based rarefaction and extrapolation: standardizing
507 samples by completeness rather than size. *Ecology* **93**, 2533–2547.
- 508 32. Alroy, J. 2018 Limits to species richness in terrestrial communities. *Ecology* **53**, 1211–
509 9. (doi:10.1111/ele.13152)
- 510 33. Chao, A. 1984 Nonparametric estimation of the number of classes in a population.
511 *Scandinavian Journal of statistics* **11**, 265–270.
- 512 34. Hsieh, T. C., Ma, K. H. & Chao, A. 2016 iNEXT: an R package for rarefaction and
513 extrapolation of species diversity (Hill numbers). *Methods in Ecology and Evolution*,
514 1–6. (doi:10.1111/2041-210X.12613)
- 515 35. Burnham, K. P., Anderson, D. R. & Anderson, D. F. 2002 *Model selection and*
516 *multimodel inference: a practical information-theoretic approach*. Springer Verlag.
- 517 36. Cao, W., Zahirovic, S., Flament, N., Williams, S., Golonka, J. & Müller, R. D. 2017
518 Improving global paleogeography since the late Paleozoic using paleobiology.
519 *Biogeosciences* **14**, 5425–5439. (doi:10.5194/bg-14-5425-2017)
- 520 37. Benton, M. J. 2015 Palaeodiversity and formation counts: redundancy or bias?
521 *Palaeontology* **58**, 1003–1029. (doi:10.1111/pala.12191)
- 522 38. Dunhill, A. M., Hannisdal, B. & Benton, M. J. 2014 Disentangling rock record bias
523 and common-cause from redundancy in the British fossil record. *Nat. Commun.* **5**,
524 4818–9. (doi:10.1038/ncomms5818)
- 525 39. Wall, P. D., Ivany, L. C. & Wilkinson, B. H. 2011 Impact of outcrop area on estimates
526 of Phanerozoic terrestrial biodiversity trends. *Geol. Soc. London Spec. Publ.* **358**, 53–
527 62. (doi:10.1144/SP358.5)
- 528 40. Peters, S. E. & Husson, J. M. 2017 Sediment cycling on continental and oceanic crust.
529 *Geology* **45**, 323–326. (doi:10.1130/g38861.1)

- 530 41. Benson, R. B. J., Mannion, P. D., Butler, R. J., Upchurch, P., Goswami, A. & Evans,
531 S. E. 2013 Cretaceous tetrapod fossil record sampling and faunal turnover:
532 Implications for biogeography and the rise of modern clades. *Palaeogeogr.*
533 *Palaeoclimatol. Palaeoecol.* **372**, 88–107. (doi:10.1016/j.palaeo.2012.10.028)
- 534 42. Clack, J. A. 2012 *Gaining Ground*. Indiana University Press.
- 535 43. Vavrek, M. J. 2016 The fragmentation of Pangaea and Mesozoic terrestrial vertebrate
536 biodiversity. *Biol. Lett.* **12**, 20160528. (doi:10.1098/rsbl.2016.0528)
- 537 44. Eriksson, O. 2014 Evolution of angiosperm seed disperser mutualisms: the timing of
538 origins and their consequences for coevolutionary interactions between angiosperms
539 and frugivores. *Biol. Rev.* **91**, 168–186. (doi:10.1111/brv.12164)
- 540 45. Clapham, M. E., Karr, J. A., Nicholson, D. B., Ross, A. J. & Mayhew, P. J. 2016
541 Ancient origin of high taxonomic richness among insects. *Proc. R. Soc. B* **283**,
542 20152476. (doi:10.1098/rspb.2015.2476)
- 543 46. Knoll, A. H. 1986 Patterns of change in plant communities through geological time. In
544 *Community Ecology* (eds J. Diamond & T. J. Case), pp. 126–141. New York: Harper
545 & Row.
- 546 47. Hyndman, R. J. & Khandakar, Y. 2008 Automatic time series forecasting: the forecast
547 package for R. *J. Stat. Soft.* **27**. (doi:10.18637/jss.v027.i03)
- 548

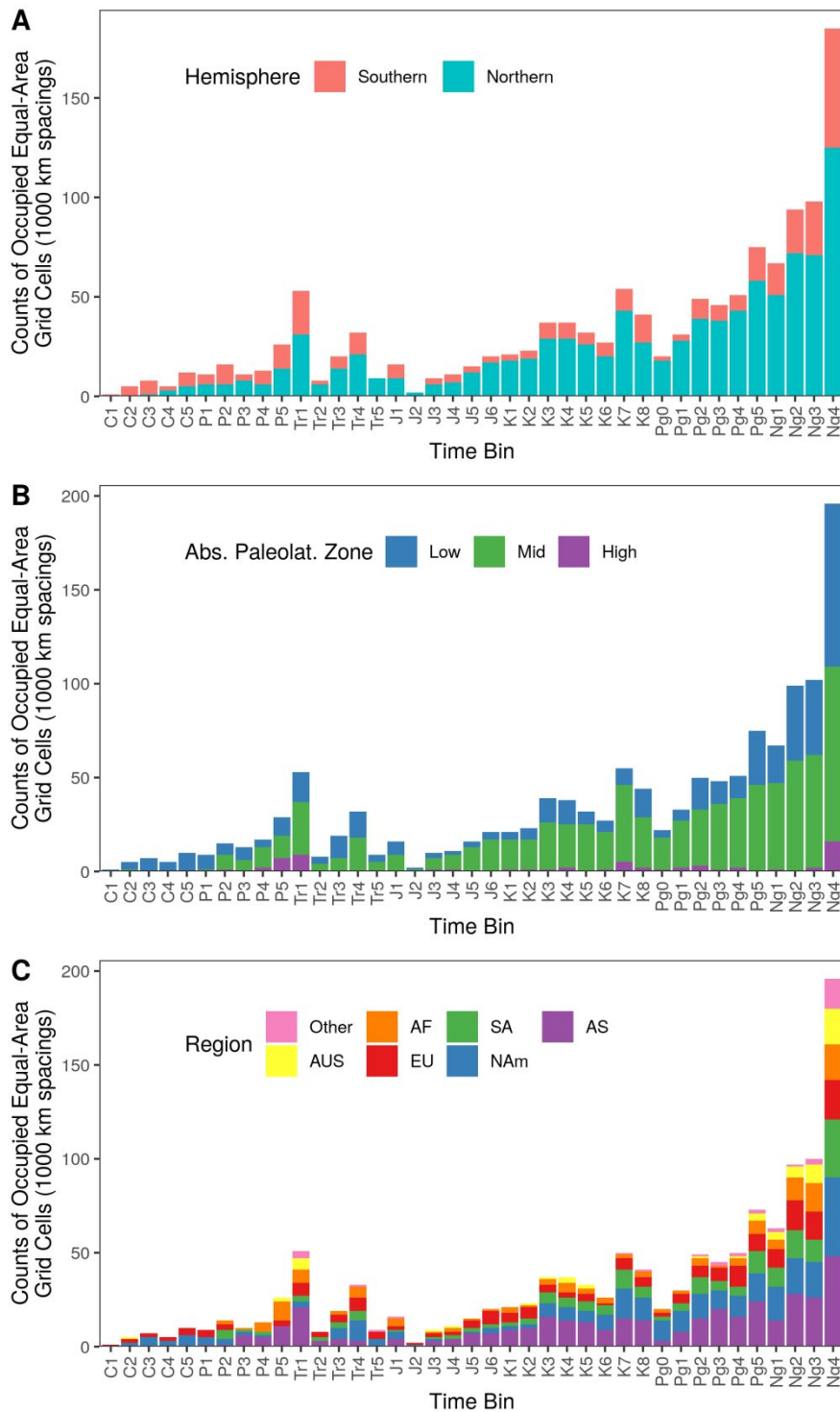
549



550

551 **Fig. 1.** Spatial bias and the global fossil record of Phanerozoic terrestrial tetrapods. (A) Face-
 552 value (red) and sampling-standardised (SQS [29,31] using quorum = 0.6; blue) ‘global’
 553 species richness of Phanerozoic terrestrial tetrapods. (B) Spatial sampling (occupied equal-
 554 area grid cells with 500 km spacings, green) and habitable area (terrestrial area as a
 555 percentage of Earth’s surface [36], purple). Counts of occupied grid cells increase steeply
 556 through the Cenozoic, and accelerate towards the present. (C, D) Relationships between
 557 changes in (B) face-value and (D) sampling-standardised species richness (using SQS,
 558 quorum = 0.6) and changes in counts of occupied grid cells per equal-length bin (all variables
 559 log-transformed). (E, F) Relationships between (E) changes in face-value and (F) sampling-
 560 standardised species richness (using SQS, quorum = 0.6) and changes in continental area
 561 through time. Datapoints for C1 and C2 removed as outliers.

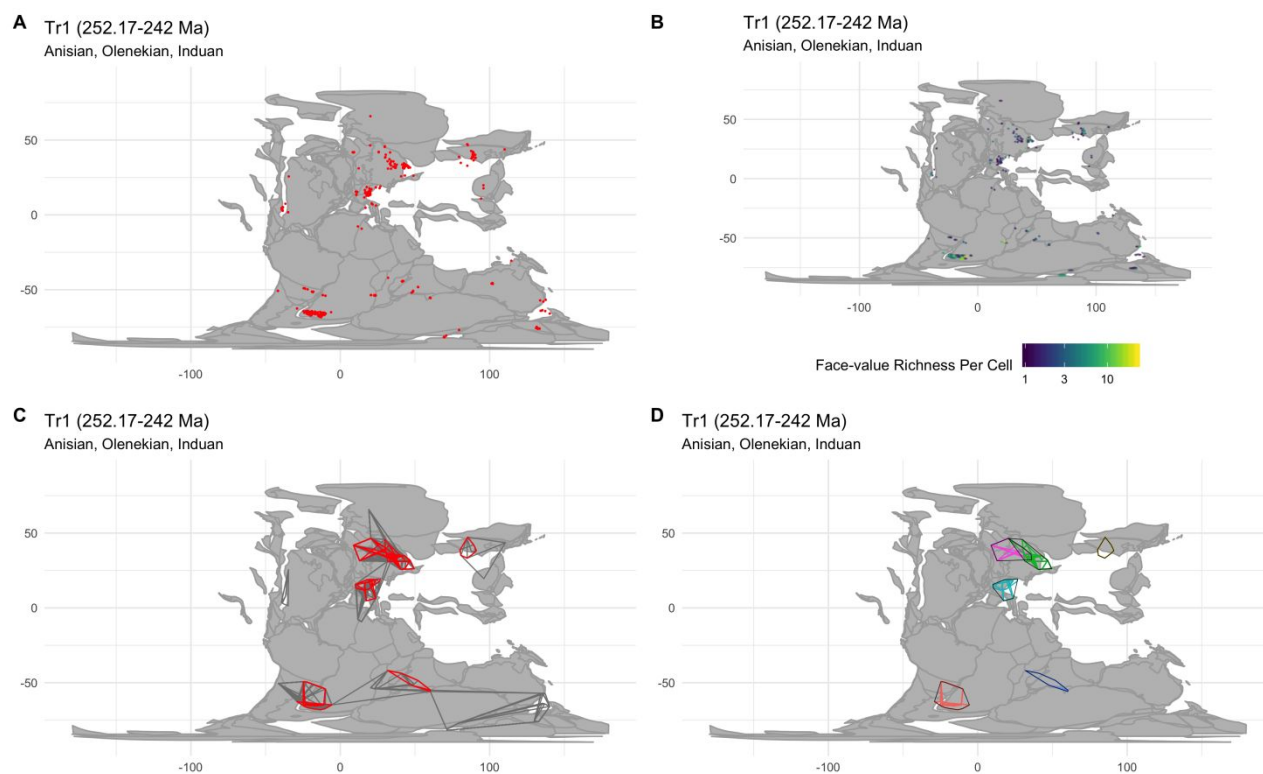
14



562

563 **Fig. 2.** Spatial sampling in the Phanerozoic record of terrestrial tetrapods. Per-bin counts of
 564 equal-area grid cells with 200 km spacings, broken down by (A) hemisphere, (B) absolute
 565 palaeolatitude zone (low = 0–30°, mid = 30–60°, high = 60–90°), and (C) continental region.
 566 Spatial sampling rises steeply through the Phanerozoic, and is especially limited outside of
 567 North America, Europe and Asia, in the southern hemisphere, and at low and high
 568 palaeolatitudes.

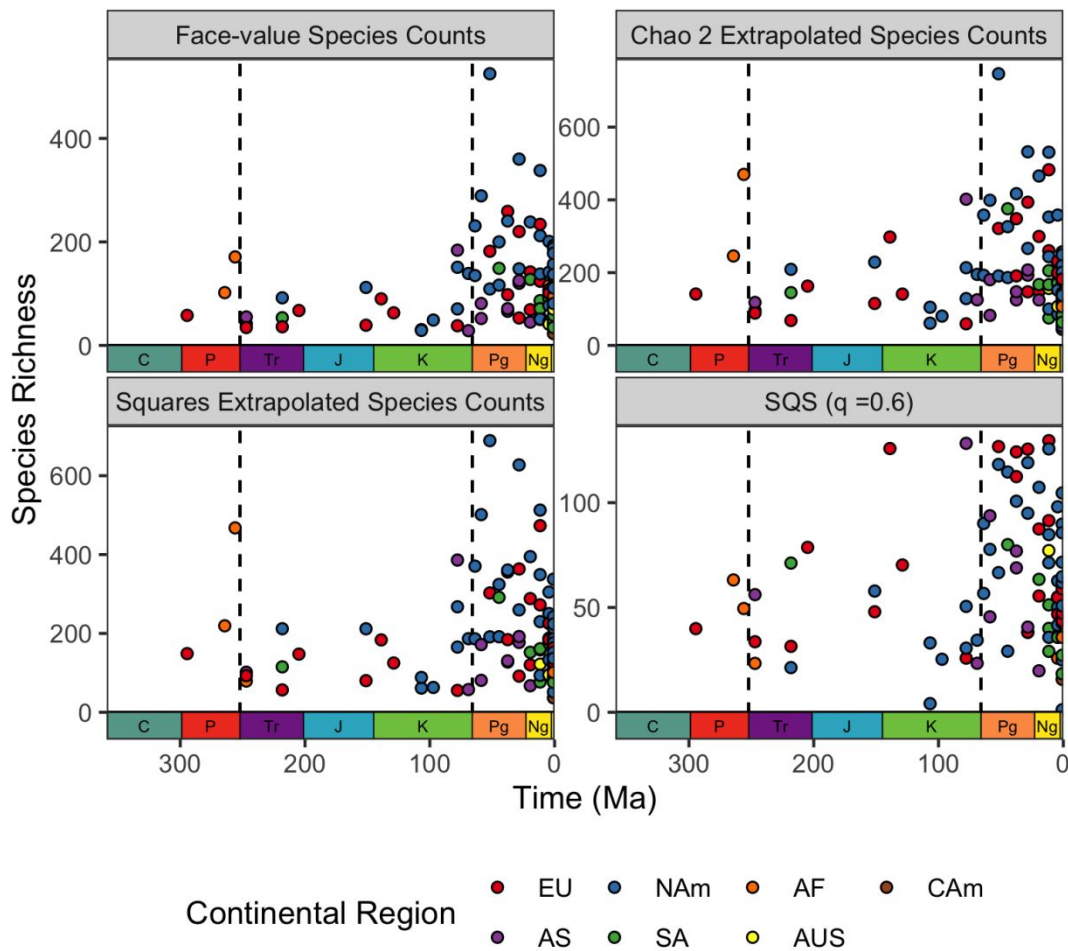
569



570

571 **Fig. 3.** Key steps in the spatial standardisation procedure used in this study, showing samples
 572 for the early–middle Triassic (Tr1 time bin). (A) Palaeocoordinates of fossil localities. (B)
 573 Fossil localities binned within 100 km equal-size hexagonal/pentagonal grid cells (using
 574 `dggridR`). (C) Palaeogeographic regions delineated using convex hulls, with samples meeting
 575 spatial standardisation criteria for 2000 km MST distance highlighted in red. (D) Clusters of
 576 highly similar palaeogeographic regions.

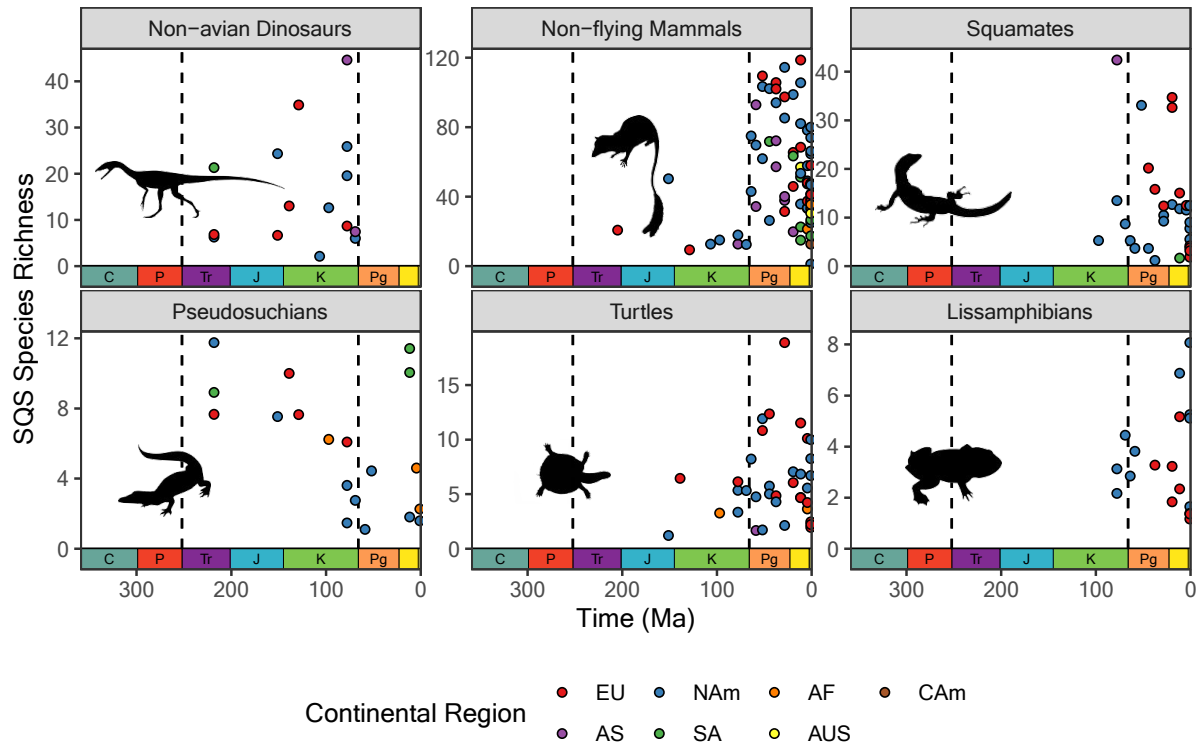
577



578

579 **Fig. 4.** Patterns of spatially-standardised regional-scale species richness of non-flying
 580 terrestrial tetrapods through the Phanerozoic, for regions 2000 km in size (minimum-
 581 spanning tree [MST] distance). Patterns depicted using face-value (but spatially standardised)
 582 species counts, squares [32] and Chao 2 extrapolated richness [33], and SQS [29,31] (using
 583 quorum = 0.6). Grid-cell rarefaction algorithm not used (GCR = off). Colours correspond to
 584 dominant continental regions of palaeogeographic regions. Data points represent median
 585 richness estimates for clustered palaeogeographic regions.

586



587

588 **Fig. 5.** Patterns of spatially-standardised regional-scale species richness for major subclades
 589 of non-flying terrestrial tetrapods (non-avian dinosaurs, non-flying mammals, squamates,
 590 pseudosuchians, turtles and lissamphibians), for regions 2000 km in size (minimum-spanning
 591 tree [MST] distance). Species richness estimates extrapolated using SQS (quorum = 0.6,
 592 GCR = off). Colours represent dominant continental regions of palaeogeographic regions.
 593 Silhouettes courtesy of Phylopic (<http://www.phylopic.org>). Image credits for Phylopic
 594 silhouettes: non-avian dinosaur by Ian Reid, CC BY-NC-SA 3.0; non-flying mammal by
 595 FunkMonk/Michael B. H. (CC BY-NC-SA 3.0); squamate by Ghedo and T. Michael Keesey
 596 (CC BY-SA 3.0); pseudosuchian by Phylopic (Public Domain Mark 1.0); turtle by Phylopic
 597 (Public Domain Dedication 1.0); lissamphibian by Nobu Tamura (CC BY 3.0).
 598

599 **Table 1.** Model selection using the second-order Akaike information criterion (AICc) to
 600 compare fits of linear models of spatially-standardised non-flying terrestrial species richness
 601 (SQS, quorum = 0.6; 1000–4000 km MST distance, GCR = off) as a function of time and
 602 diversification phase.

model	df	logLik	AICc	delta AICc	weights	cumulative weights	evidence ratio
1000 km summed MST distance							
Time * Phase	4	-71.6	154	0.00	5.86e-01	0.586	1.00
Phase Only	2	-74.5	155	1.47	2.81e-01	0.867	2.09
Time + Phase	3	-74.2	157	3.08	1.25e-01	0.992	4.69
Time Only	2	-78.1	162	8.68	7.64e-03	1.000	76.70
Intercept Only	1	-82.5	169	15.40	2.66e-04	1.000	2200.00
1500 km summed MST distance							
Time * Phase	4	-86.3	183	0.00	9.29e-01	0.929	1.00
Phase Only	2	-91.7	189	6.30	3.99e-02	0.969	23.30
Time + Phase	3	-91.0	190	7.05	2.74e-02	0.996	33.90
Time Only	2	-94.4	195	11.70	2.63e-03	0.999	353.00
Intercept Only	1	-96.2	196	13.30	1.22e-03	1.000	761.00
2000 km summed MST distance							
Time * Phase	4	-90.4	191	0.00	7.99e-01	0.799	1.00
Time + Phase	3	-93.6	195	4.05	1.05e-01	0.904	7.61
Phase Only	2	-95.2	197	5.26	5.76e-02	0.962	13.90
Intercept Only	1	-97.0	198	6.78	2.69e-02	0.988	29.70
Time Only	2	-96.9	200	8.51	1.13e-02	1.000	70.70
2500 km summed MST distance							
Time * Phase	4	-68.5	148	0.00	9.92e-01	0.992	1.00
Time + Phase	3	-74.9	158	10.40	5.38e-03	0.997	184.00

model	df	logLik	AICc	delta AICc	weights	cumulative weights	evidence ratio
Phase Only	2	-76.7	160	12.00	2.45e-03	1.000	405.00
Intercept Only	1	-81.5	167	19.50	5.74e-05	1.000	17300.00
Time Only	2	-80.5	167	19.70	5.35e-05	1.000	18500.00
3000 km summed MST distance							
Time * Phase	4	-59.4	129	0.00	9.45e-01	0.945	1.00
Time + Phase	3	-63.6	136	6.10	4.47e-02	0.990	21.10
Phase Only	2	-66.1	138	9.00	1.05e-02	1.000	90.00
Time Only	2	-71.4	149	19.50	5.45e-05	1.000	17300.00
Intercept Only	1	-73.4	151	21.40	2.12e-05	1.000	44600.00
3500 km summed MST distance							
Time * Phase	4	-51.6	114	0.00	9.63e-01	0.963	1.00
Time + Phase	3	-56.3	121	7.21	2.61e-02	0.989	36.90
Phase Only	2	-58.3	123	8.96	1.09e-02	1.000	88.30
Time Only	2	-63.5	133	19.30	6.08e-05	1.000	15800.00
Intercept Only	1	-65.6	135	21.40	2.12e-05	1.000	45400.00
4000 km summed MST distance							
Time * Phase	4	-52.9	116	0.00	9.64e-01	0.964	1.00
Phase Only	2	-59.0	124	7.81	1.94e-02	0.983	49.70
Time + Phase	3	-58.1	125	8.12	1.66e-02	1.000	58.10
Time Only	2	-63.5	133	16.80	2.22e-04	1.000	4340.00
Intercept Only	1	-66.3	137	20.30	3.83e-05	1.000	25200.00

604 **Table 2.** Coefficients for variables included in generalised least-squares models of ‘global’
 605 species richness (face-value and sampling standardised, using SQS at a quorum of 0.6) as a
 606 function of the palaeogeographic spread of the fossil record (counts of occupied equal-area
 607 grid cells with 500 km spacings), continental area and non-marine sediment extent (counts of
 608 columns in Macrostrat database). Temporally-correlated errors modelled using a first-order
 609 autoregressive structure. Palaeogeographic spread and non-marine sediment extent variables
 610 log-transformed to achieve normality. When all three explanatory variables are included in a
 611 linear model, only palaeogeographic spread (MST distance) is a significant (at $p \leq 0.01$) and
 612 strong explanation of variation in ‘global’ species richness.

term	estimate	std.error	statistic	p.value
Face-value Global Species Richness				
Intercept	-2.1600	1.8300	-1.1900	n.s.
Occupied Grid Cells	0.8340	0.0960	8.6900	< 0.01
Non-marine Sediment Extent	-0.0256	0.1720	-0.1490	n.s.
Continental Area	0.1820	0.0785	2.3100	n.s.
SQS Global Richness				
Intercept	2.4500	1.6600	1.4700	n.s.
Occupied Grid Cells	0.5010	0.1240	4.0400	< 0.01
Non-marine Sediment Extent	-0.0143	0.1880	-0.0761	n.s.
Continental Area	0.0413	0.0777	0.5310	n.s.

613

614 **Supplementary Information**

615 **Supplementary Methods**

616 *Note on spatial subsampling procedure.* We use the spatial distribution of fossil localities
617 with well-defined palaeocoordinates to quantify the palaeogeographic extent of the known
618 fossil record for each interval. The strength of the correlation between geographic spread and
619 estimated richness is very great (Figs 1 and S6), and is unlikely to be the result of errors.
620 Minor errors would primarily arise from recording modern-day geographic coordinates
621 inaccurately in the Paleobiology Database, and from tectonic rotations used to recover
622 palaeocoordinates. However, for most of the standardised palaeogeographic regions that we
623 analyse (i.e., subsamples of fossil localities with approximately equal geographic extents), the
624 localities come from regions of the globe that are linked on a single tectonic plate that moves
625 as a rigid unit. Therefore, the error associated with these estimates are, for our purposes,
626 negligible.

627 **Supplementary Results**

628 *Model-fitting with additional richness estimators.* Model-selection and fitting results for other
629 richness estimators are given in Tables S3–S4 (SQS with GCR), S5–S6 (face-value species
630 counts), S7–S8 (squares) and S9–S10 (Chao 2). Results are highly congruent for all richness
631 estimators, with the “Time * Pre/Post-K/Pg phase” model receiving highest support. In all
632 models that include phase and time as an interaction term, this is due to a significant decrease
633 in richness through the Cenozoic (Tables S6, S8 and S10; Fig. S9).

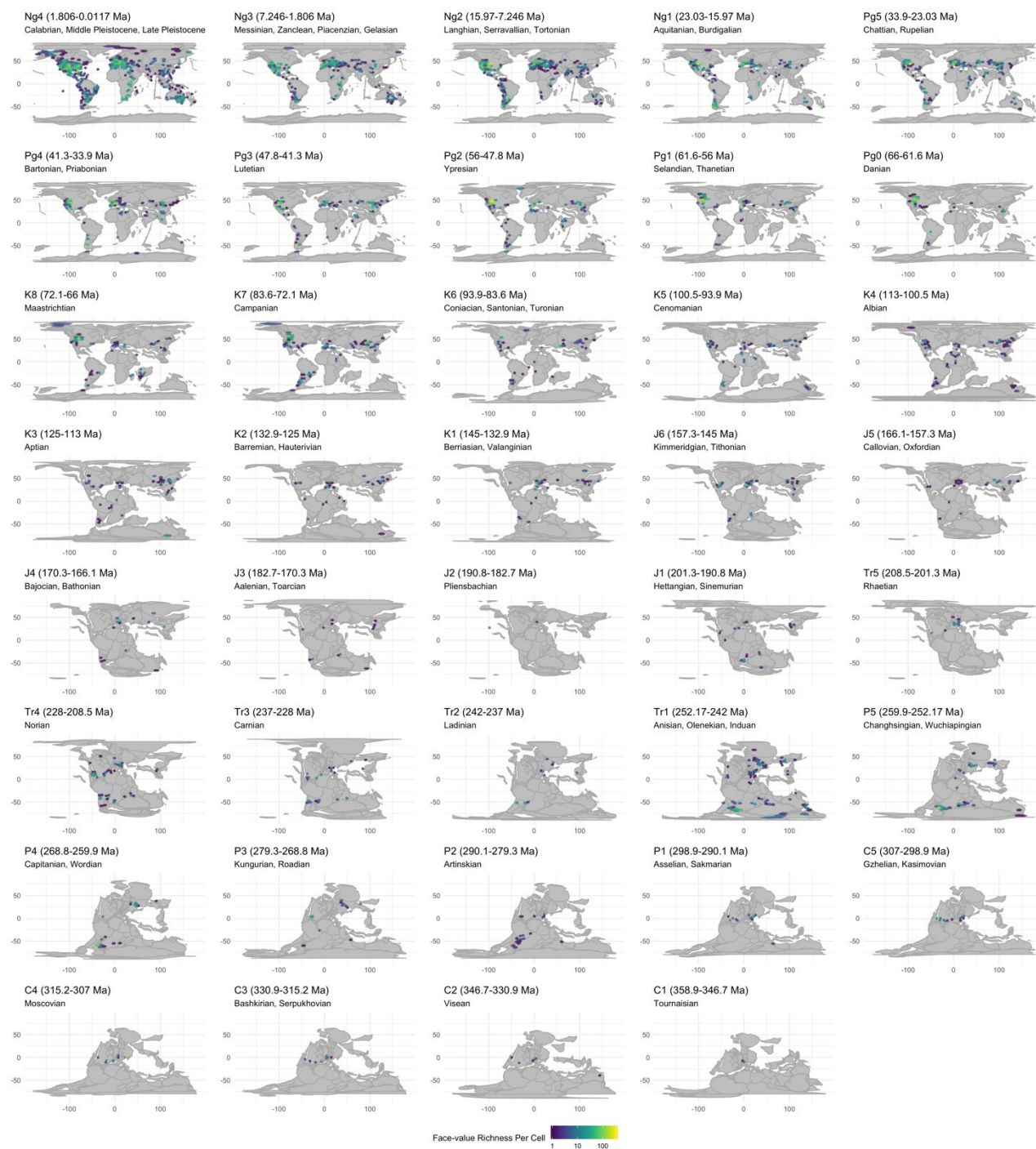
634



635

636 **Fig. S1.** Distribution of non-flying tetrapod fossil localities through the Phanerozoic, using
 637 equal-length time bins.

638



639

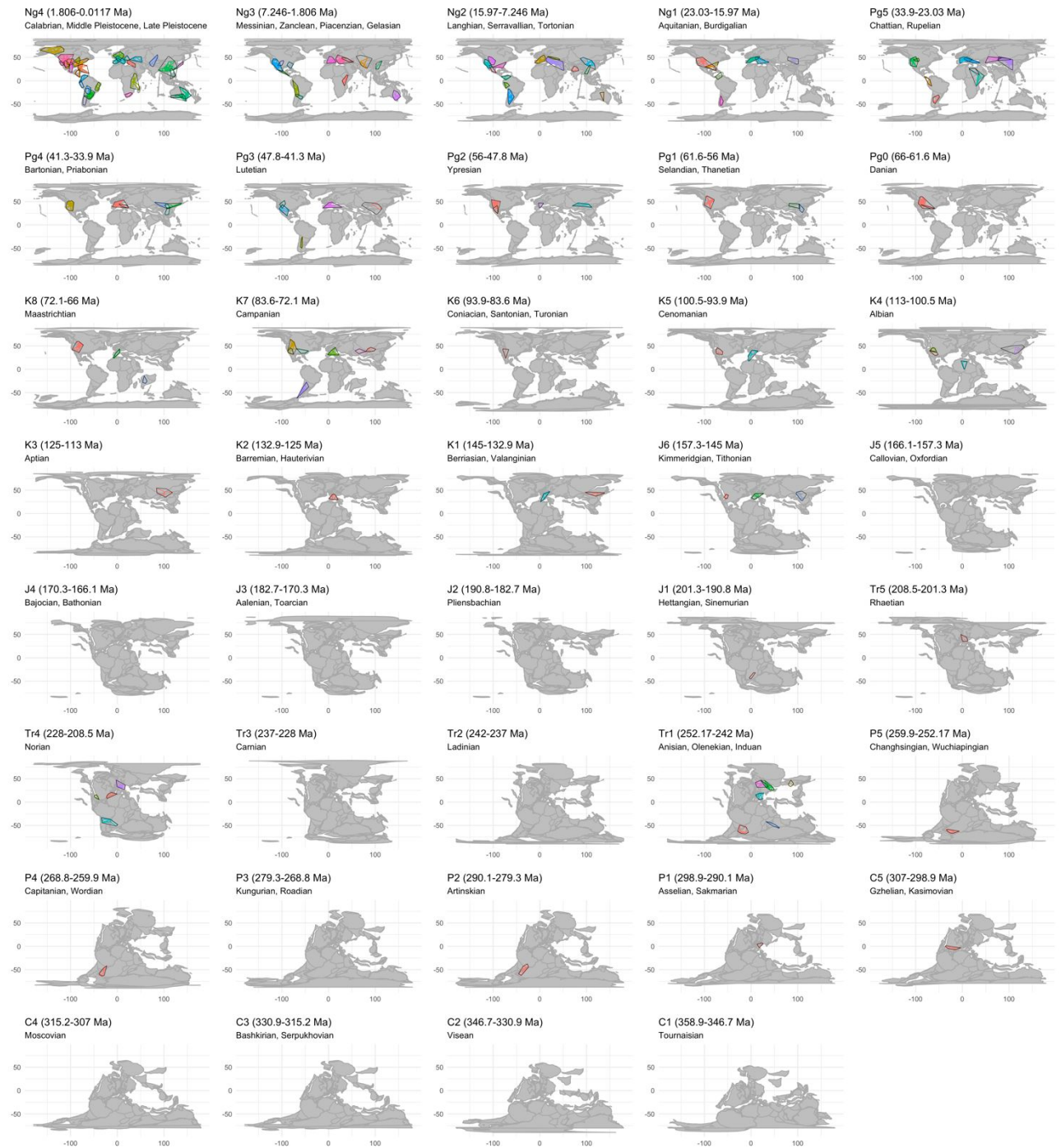
640 **Fig. S2.** Distribution of equal-sized hexagonal/pentagonal grid cells with 500 km spacings
 641 (between cell midpoints) containing occurrences of non-flying tetrapod fossils through the
 642 Phanerozoic, using equal-length time bins. Colours represent face-value species counts per
 643 cell.



645

646 **Fig. S3.** Distribution of subsampled spatial regions sampling non-flying tetrapod fossils
 647 through the Phanerozoic, using equal-length time bins. Spatial regions meeting spatial
 648 standardisation criteria for 2000 km MST lengths (see Methods for full list of criteria) are in
 649 red, and those not meeting these criteria are in grey.

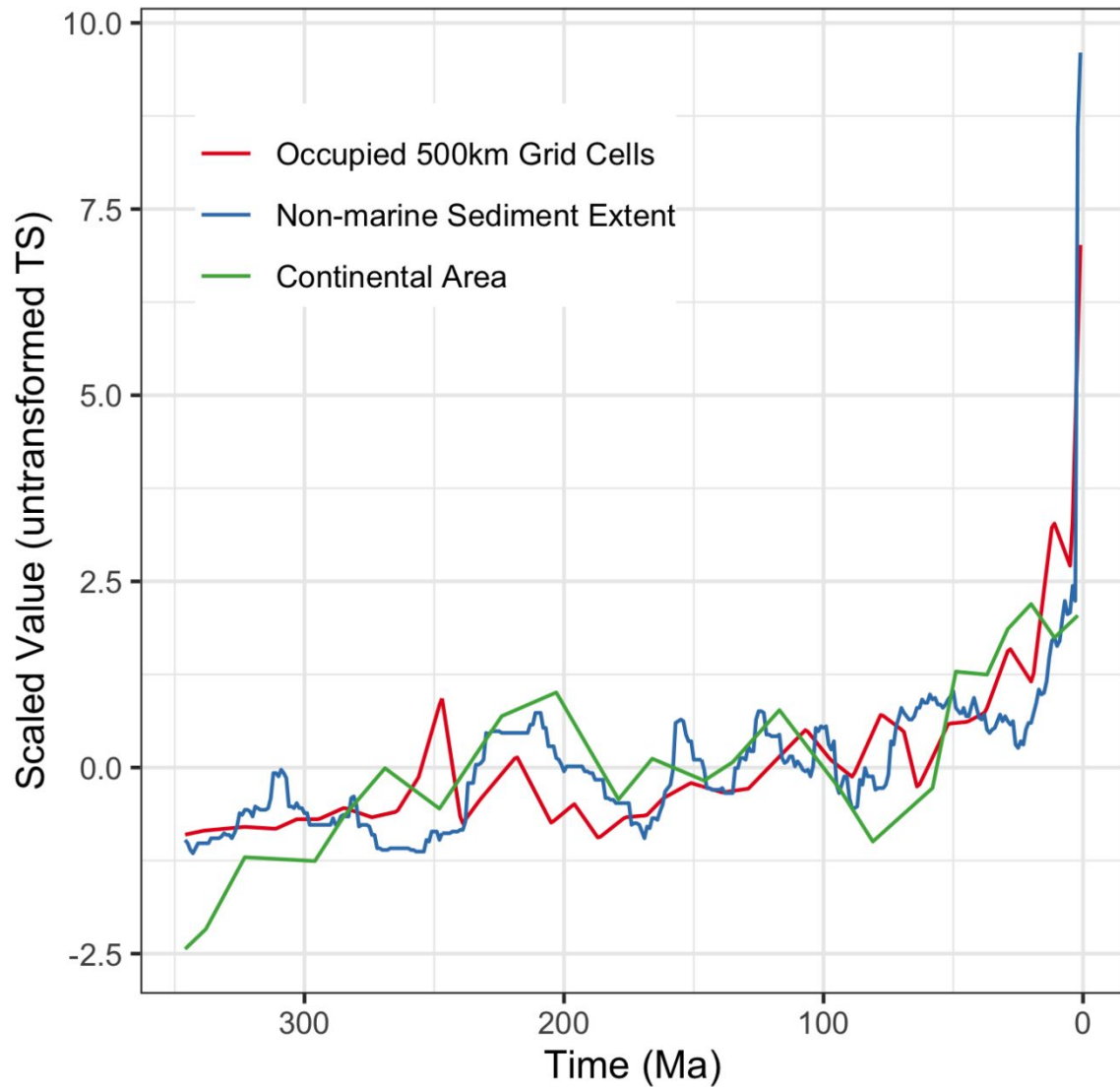
650



651

652 **Fig. S4.** Clusters of subsampled spatial regions (2000 km MST length) for non-flying
 653 tetrapods through the Phanerozoic, using equal-length time bins. Colours differentiate
 654 clusters.

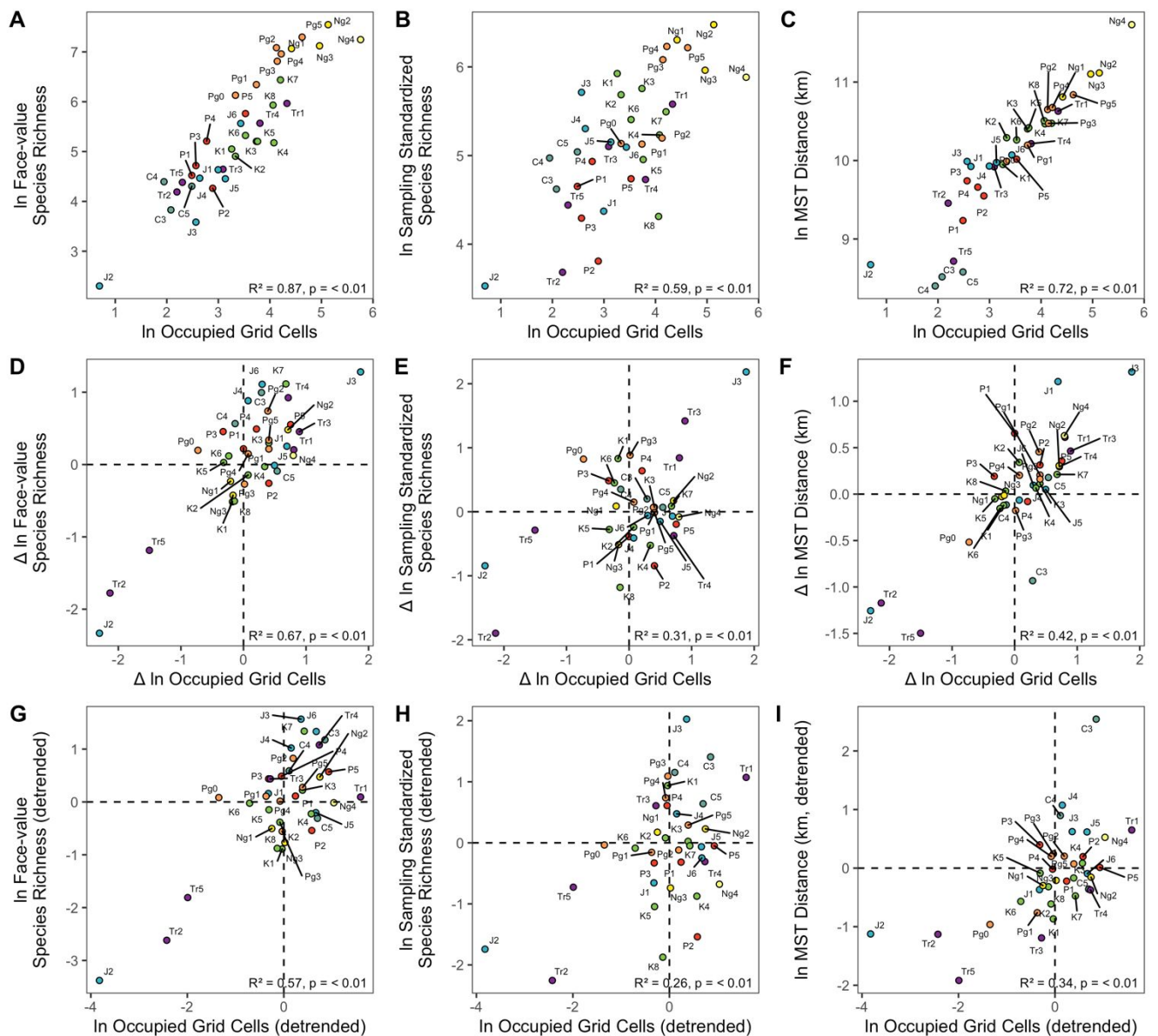
655



656

657 **Fig. S5.** Time series (scaled to unit variance and centred) for the palaeogeographic spread of
 658 the worldwide non-flying terrestrial tetrapod fossil record (occupied equal-area grid cells
 659 with 500 km spacings), and estimates of continental area (from Cao et al. [36]) and non-
 660 marine sediment extent (derived from Macrostrat by [40]). Only non-marine sediment extent
 661 mirrors palaeogeographic spread in rising sharply during the Neogene–Recent, and increases
 662 in continental area over the same interval are much smaller.

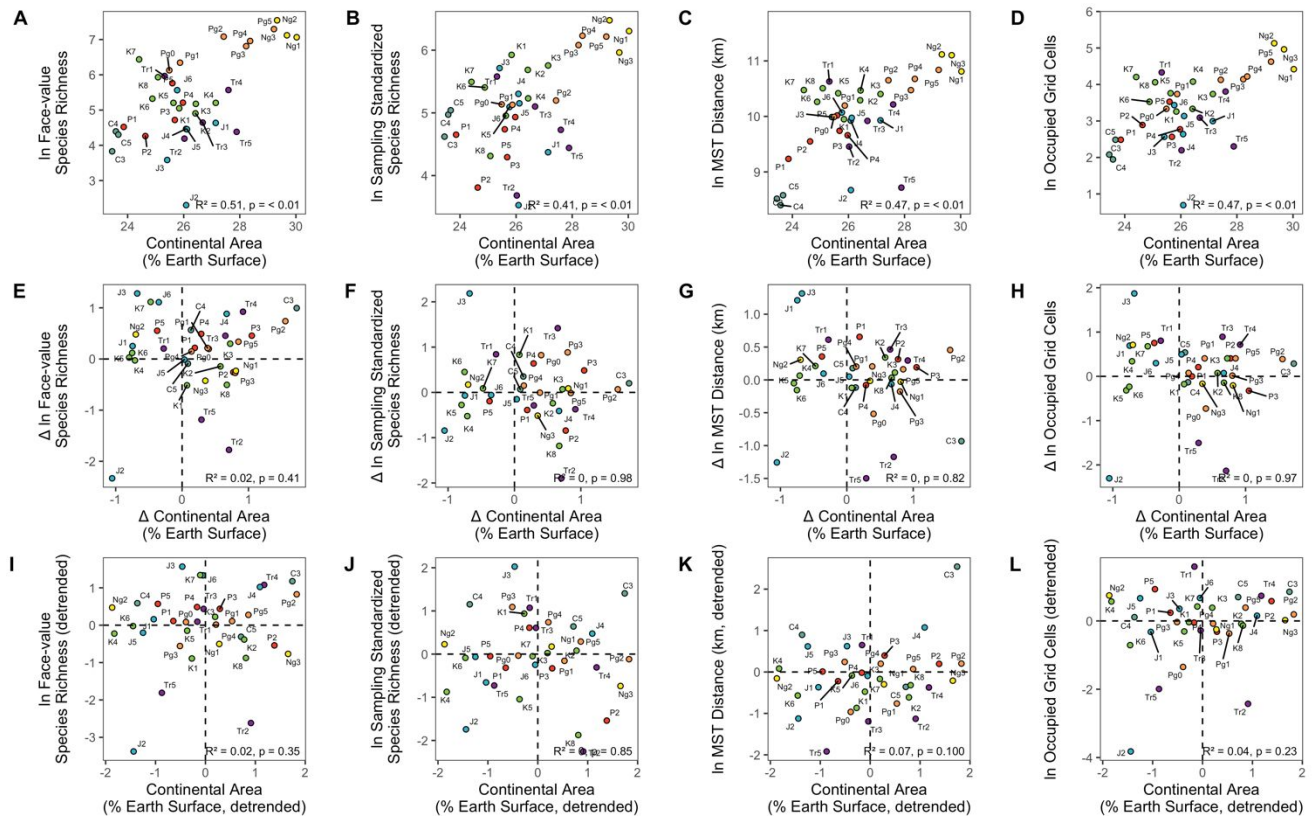
663



664

665 **Fig. S6.** Bivariate relationships between the palaeogeographic spread of the worldwide non-
 666 marine, non-flying tetrapod fossil record, quantified using per-bin counts of occupied equal-
 667 area grid cells with 500 km spacings ([36]) and other key variables. (A–B) Raw (i.e. not
 668 detrended or differenced) relationships between time series occupied grid cell counts and
 669 “global” tetrapod species richness estimates (face-value counts of species, and sampling
 670 standardised SQS richness at quorum = 0.6). (D–E) Corresponding first-differenced
 671 relationships. (G–H) Corresponding relationships for time series detrended with ARIMA
 672 models (using the R function `auto.arima()` in the package `forecast` [47]). (C, F, I)
 673 Relationships between palaeogeographic spread quantified using occupied grid cells, and
 674 using MST length. All variables log-transformed. Datapoints for C1 and C2 removed as
 675 outliers.

676

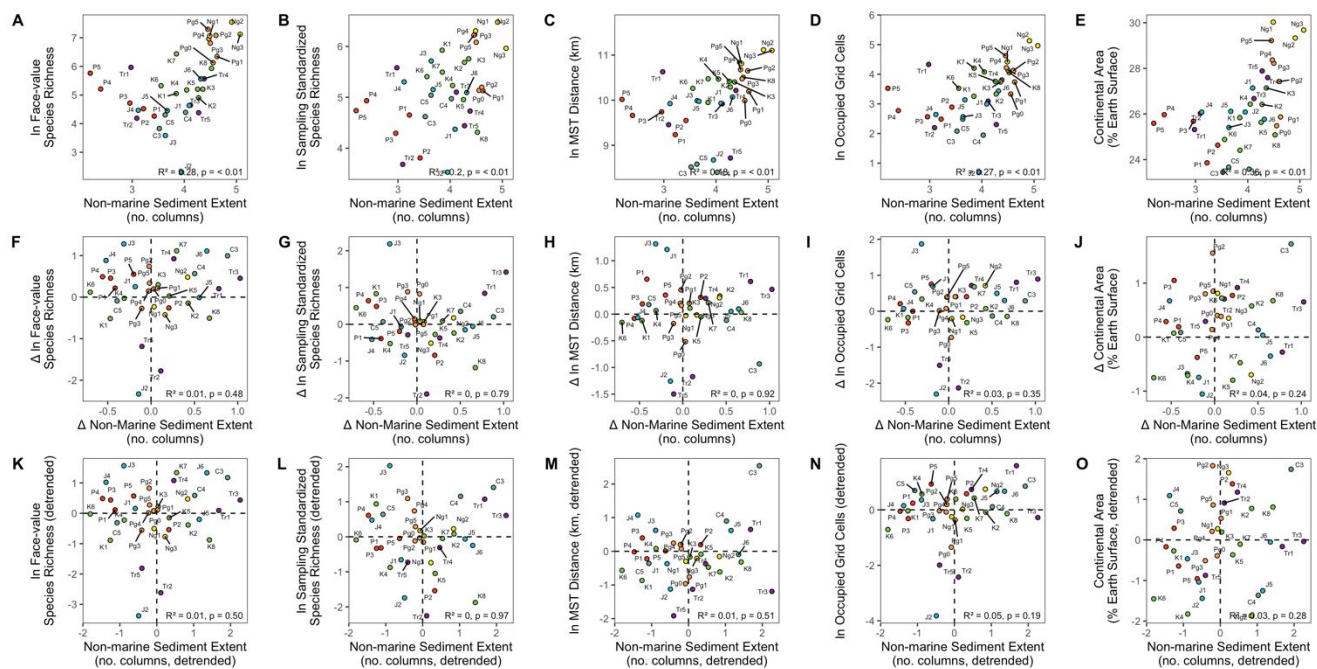


677

678 **Fig. S7.** Bivariate relationships between an estimate of continental area through the
 679 Phanerozoic ([36]) and other key variables. (A–D) Raw (i.e. not detrended or differenced)
 680 relationships between time series of continental area, “global” tetrapod species richness
 681 estimates, and the palaeogeographic spread of their fossil record. (E–H) Corresponding first-
 682 differenced relationships. (I–L) Corresponding relationships for time series detrended with
 683 ARIMA models (using the R function `auto.arima()` in the package `forecast` [47]). Datapoints
 684 for C1 and C2 removed as outliers. Although relationships using ‘raw’ time series are
 685 significant, accounting for spurious time series effects renders them non-significant.

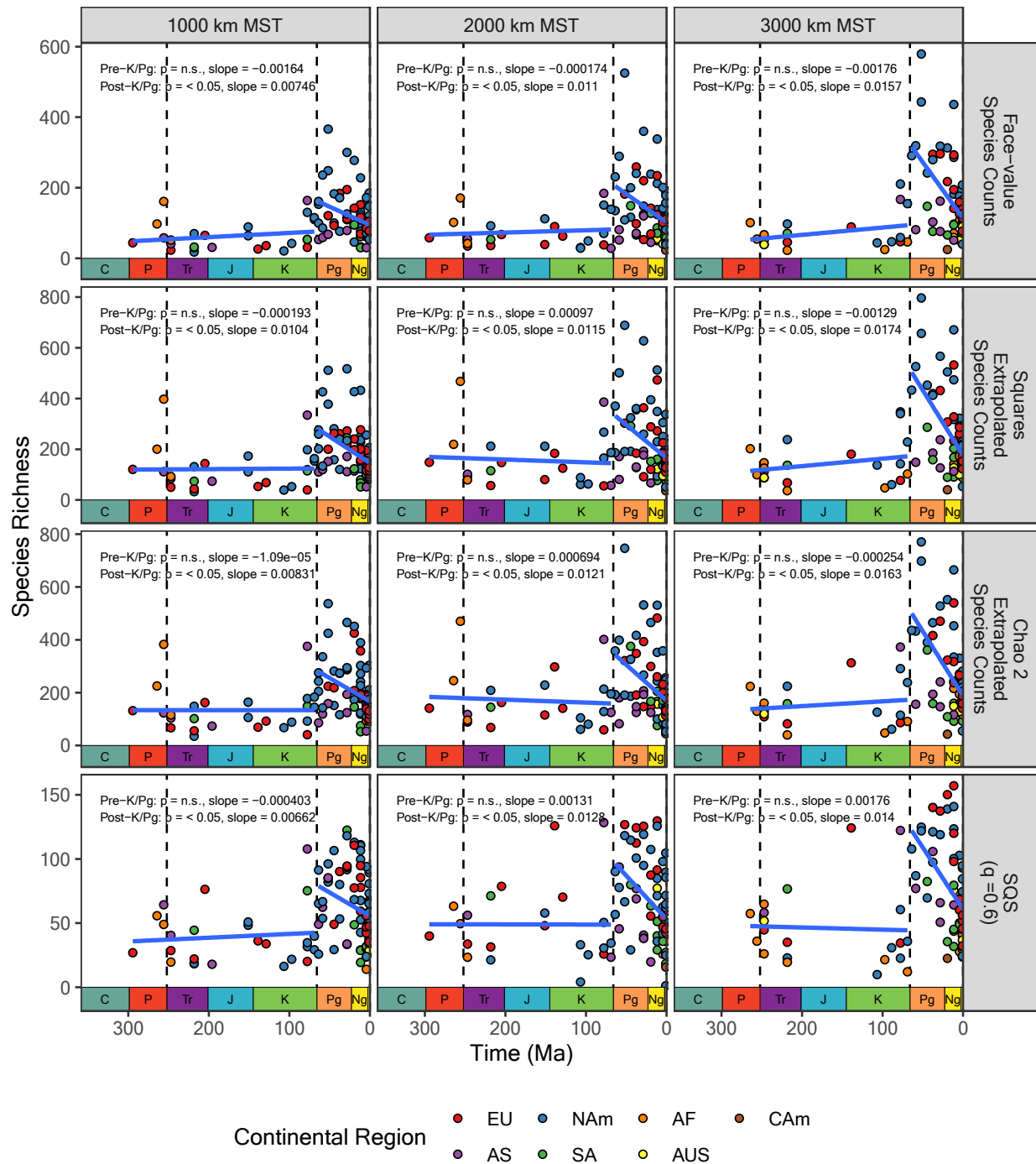
686

687



688

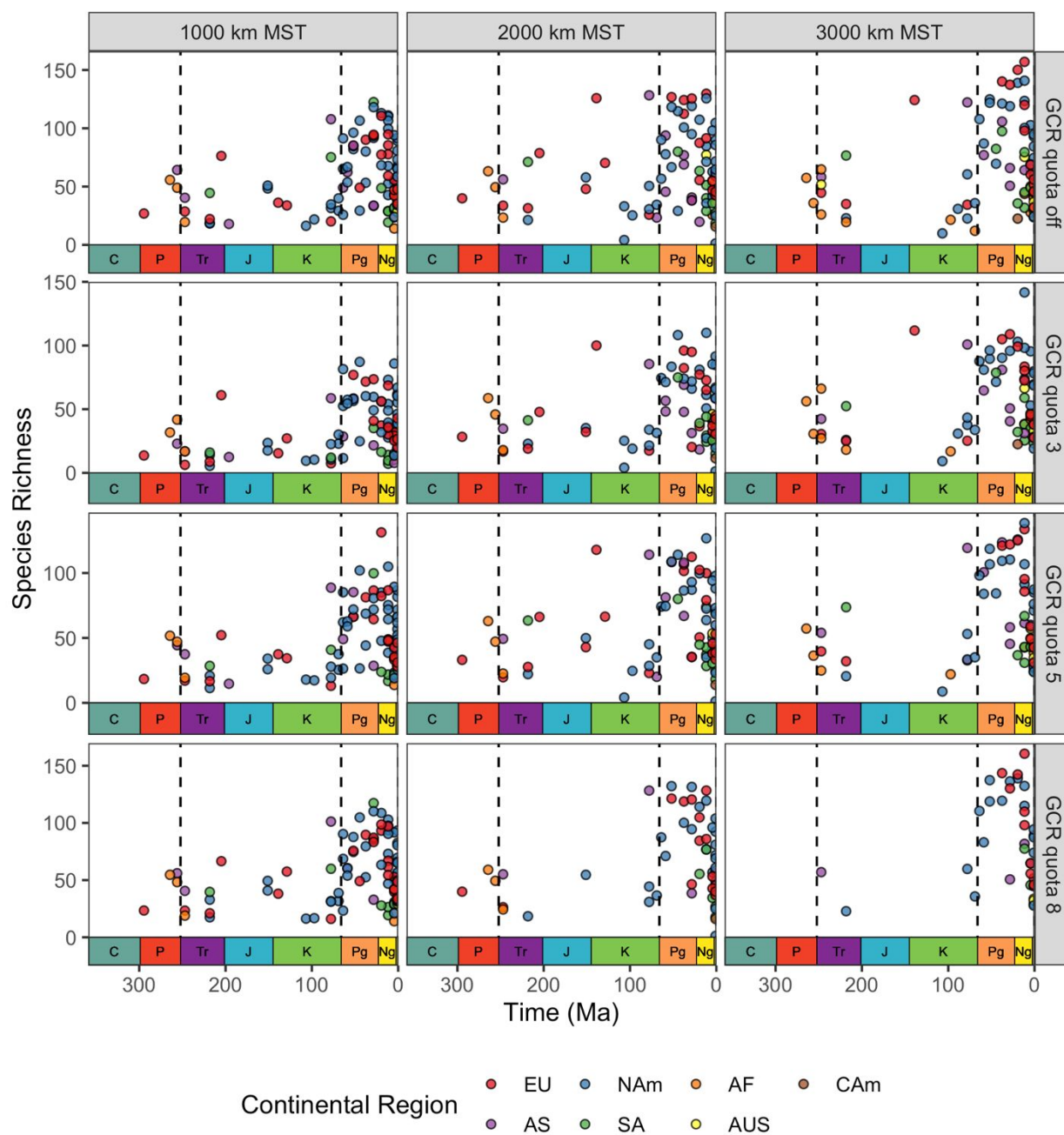
689 **Fig. S8.** Bivariate relationships between non-marine sediment extent (derived from the
 690 Macrostrat database (<http://www.macrostrat.org>), via Peters and Husson [40]) and other key
 691 variables. (A–E) Raw (i.e. not detrended or differenced) relationships between time series of
 692 non-marine sediment extent and diversity, palaeogeographic spread and continental area. (F–
 693 J) Corresponding first-differenced relationships. (K–O) Corresponding relationships for time
 694 series detrended with ARIMA models (using the R function `auto.arima()` in the package
 695 `forecast` [47]). Datapoints for C1 and C2 removed as outliers. Although relationships using
 696 ‘raw’ time series are significant, accounting for spurious time series effects renders them
 697 non-significant.



699

700 **Fig. S9.** Linear models of ln richness as a function of time within pre- and post-K/Pg
 701 diversification phases, for face-value species counts (= raw or uncorrected richness; i.e., not
 702 sampling-standardised), squares' extrapolated species richness and SQS richness (quorum =
 703 0.6). No grid-cell rarefaction used (GCR = off). Shaded envelopes denote 95% confidence
 704 intervals for regression slopes. Regressions for the pre-K/Pg phase are never significant, but
 705 those for the post-K/Pg phase are sometimes significant, with a positive slope (indicating a
 706 statistically significant decline in diversity towards the present).

707



708

709 **Fig. S10.** Effects of using a grid-cell rarefaction procedure (using quotas of 3, 5 and
 710 occupied cells per 1000 km of summed MST distance) prior to computing SQS richness
 711 estimates (quorum = 0.6) on spatially-standardised regions. GCR algorithm not used for
 712 “GCR quota = off”. As the GCR quota is raised, increasingly fewer suitable regions are
 713 available from pre-Cenozoic intervals.

714

715 **Supplementary Tables**716 **Table S1.**

717 Definitions of composite time bins of approximately equal length.

bin	stages	LAD	FAD	midpoint	duration
Ng4	Calabrian, Middle Pleistocene, Late Pleistocene	0.0117	1.806	0.90885	1.7943
Ng3	Messinian, Zanclean, Piacenzian, Gelasian	1.8060	7.246	4.52600	5.4400
Ng2	Langhian, Serravallian, Tortonian	7.2460	15.970	11.60800	8.7240
Ng1	Aquitanian, Burdigalian	15.9700	23.030	19.50000	7.0600
Pg5	Chattian, Rupelian	23.0300	33.900	28.46500	10.8700
Pg4	Bartonian, Priabonian	33.9000	41.300	37.60000	7.4000
Pg3	Lutetian	41.3000	47.800	44.55000	6.5000
Pg2	Ypresian	47.8000	56.000	51.90000	8.2000
Pg1	Selandian, Thanetian	56.0000	61.600	58.80000	5.6000
Pg0	Danian	61.6000	66.000	63.80000	4.4000
K8	Maastrichtian	66.0000	72.100	69.05000	6.1000
K7	Campanian	72.1000	83.600	77.85000	11.5000
K6	Coniacian, Santonian, Turonian	83.6000	93.900	88.75000	10.3000
K5	Cenomanian	93.9000	100.500	97.20000	6.6000
K4	Albian	100.5000	113.000	106.75000	12.5000
K3	Aptian	113.0000	125.000	119.00000	12.0000
K2	Barremian, Hauterivian	125.0000	132.900	128.95000	7.9000
K1	Berriasian, Valanginian	132.9000	145.000	138.95000	12.1000
J6	Kimmeridgian, Tithonian	145.0000	157.300	151.15000	12.3000
J5	Callovian, Oxfordian	157.3000	166.100	161.70000	8.8000
J4	Bajocian, Bathonian	166.1000	170.300	168.20000	4.2000
J3	Aalenian, Toarcian	170.3000	182.700	176.50000	12.4000
J2	Pliensbachian	182.7000	190.800	186.75000	8.1000
J1	Hettangian, Sinemurian	190.8000	201.300	196.05000	10.5000
Tr5	Rhaetian	201.3000	208.500	204.90000	7.2000
Tr4	Norian	208.5000	228.000	218.25000	19.5000
Tr3	Carnian	228.0000	237.000	232.50000	9.0000
Tr2	Ladinian	237.0000	242.000	239.50000	5.0000
Tr1	Anisian, Olenekian, Induan	242.0000	252.170	247.08500	10.1700
P5	Changhsingian, Wuchiapingian	252.1700	259.900	256.03500	7.7300
P4	Capitanian, Wordian	259.9000	268.800	264.35000	8.9000
P3	Kungurian, Roadian	268.8000	279.300	274.05000	10.5000
P2	Artinskian	279.3000	290.100	284.70000	10.8000
P1	Asselian, Sakmarian	290.1000	298.900	294.50000	8.8000

C5	Gzhelian, Kasimovian	298.9000	307.000	302.95000	8.1000
C4	Moscovian	307.0000	315.200	311.10000	8.2000
C3	Bashkirian, Serpukhovian	315.2000	330.900	323.05000	15.7000
C2	Visean	330.9000	346.700	338.80000	15.8000
C1	Tournaisian	346.7000	358.900	352.80000	12.2000

718

719

Table S2. Parameter estimates for coefficients in linear models fitted to spatially-standardised terrestrial tetrapod species richness data (SQS, quorum = 0.6; 1000–4000 km MST distance; GCR quota = off). All models fitted to each palaeogeographic spread level are shown, regardless of Akaike weight, and ordering does not reflect importance.

model	Intercept				Time				Time : Phase (Pre-K/Pg)				Phase (Pre-K/Pg)			
	estimate	std.error	statistic	p.value	estimate	std.error	statistic	p.value	estimate	std.error	statistic	p.value	estimate	std.error	statistic	p.value
1000 km summed MST distance																
Intercept Only	3.90	0.0534	73.1	< 0.05												
Phase Only	4.02	0.0574	70.0	< 0.05									-0.471	0.114	-4.12	< 0.05
Time Only	4.01	0.0636	63.0	< 0.05	-0.002	0.000665	-3	< 0.05								
Time + Phase	4.00	0.0617	64.9	< 0.05	0.000851	0.00121	0.705	n.s.					-0.599	0.215	-2.79	< 0.05
Time * Phase	3.89	0.0764	51.0	< 0.05	0.00662	0.0028	2.37	< 0.05	-0.00703	0.00309	-2.27	< 0.05	-0.281	0.252	-1.11	n.s.
1500 km summed MST distance																
Intercept Only	3.95	0.0710	55.7	< 0.05												
Phase Only	4.06	0.0762	53.3	< 0.05									-0.515	0.169	-3.05	< 0.05
Time Only	4.04	0.0834	48.4	< 0.05	-0.00184	0.000969	-1.9	n.s.								
Time + Phase	4.02	0.0810	49.7	< 0.05	0.00204	0.00176	1.16	n.s.					-0.823	0.314	-2.62	< 0.05
Time * Phase	3.84	0.0981	39.2	< 0.05	0.0135	0.00412	3.28	< 0.05	-0.0138	0.00452	-3.05	< 0.05	-0.258	0.353	-0.73	n.s.
2000 km summed MST distance																
Intercept Only	3.93	0.0754	52.1	< 0.05												

model	Intercept				Time				Time : Phase (Pre-K/Pg)				Phase (Pre-K/Pg)			
	estimate	std.error	statistic	p.value	estimate	std.error	statistic	p.value	estimate	std.error	statistic	p.value	estimate	std.error	statistic	p.value
Phase Only	4.01	0.0861	46.6	< 0.05									-0.323	0.17	-1.9	n.s.
Time Only	3.96	0.0938	42.2	< 0.05	-0.000599	0.001	-0.596	n.s.								
Time + Phase	3.95	0.0910	43.4	< 0.05	0.00323	0.00178	1.82	n.s.					-0.791	0.307	-2.57	< 0.05
Time * Phase	3.78	0.1130	33.4	< 0.05	0.0128	0.00423	3.03	< 0.05	-0.0115	0.00464	-2.48	< 0.05	-0.302	0.357	-0.846	n.s.
2500 km summed MST distance																
Intercept Only	3.98	0.0655	60.8	< 0.05												
Phase Only	4.11	0.0743	55.3	< 0.05									-0.431	0.137	-3.15	< 0.05
Time Only	4.05	0.0802	50.5	< 0.05	-0.00111	0.000798	-1.39	n.s.								
Time + Phase	4.07	0.0759	53.6	< 0.05	0.00247	0.00129	1.92	n.s.					-0.789	0.23	-3.42	< 0.05
Time * Phase	3.86	0.0915	42.2	< 0.05	0.0158	0.00389	4.06	< 0.05	-0.0147	0.00409	-3.6	< 0.05	-0.354	0.247	-1.43	n.s.
3000 km summed MST distance																
Intercept Only	4.05	0.0707	57.2	< 0.05												
Phase Only	4.20	0.0758	55.4	< 0.05									-0.576	0.146	-3.94	< 0.05
Time Only	4.14	0.0851	48.7	< 0.05	-0.00174	0.00087	-2	< 0.05								
Time + Phase	4.15	0.0775	53.5	< 0.05	0.00329	0.00147	2.24	< 0.05					-1.07	0.264	-4.07	< 0.05
Time * Phase	3.98	0.0946	42.0	< 0.05	0.014	0.00396	3.53	< 0.05	-0.0122	0.00423	-2.89	< 0.05	-0.648	0.292	-2.22	< 0.05

model	Intercept				Time				Time : Phase (Pre-K/Pg)				Phase (Pre-K/Pg)			
	estimate	std.error	statistic	p.value	estimate	std.error	statistic	p.value	estimate	std.error	statistic	p.value	estimate	std.error	statistic	p.value
3500 km summed MST distance																
Intercept Only	4.13	0.0650	63.5	< 0.05												
Phase Only	4.29	0.0718	59.7	< 0.05									-0.509	0.129	-3.96	< 0.05
Time Only	4.22	0.0795	53.1	< 0.05	-0.00151	0.000736	-2.06	< 0.05								
Time + Phase	4.25	0.0732	58.0	< 0.05	0.00237	0.00121	1.96	n.s.					-0.876	0.225	-3.88	< 0.05
Time * Phase	4.07	0.0895	45.5	< 0.05	0.013	0.00364	3.58	< 0.05	-0.0118	0.00384	-3.09	< 0.05	-0.501	0.245	-2.04	< 0.05
4000 km summed MST distance																
Intercept Only	4.17	0.0751	55.5	< 0.05												
Phase Only	4.35	0.0824	52.8	< 0.05									-0.583	0.147	-3.97	< 0.05
Time Only	4.30	0.0912	47.2	< 0.05	-0.00197	0.000824	-2.39	< 0.05								
Time + Phase	4.32	0.0852	50.7	< 0.05	0.00186	0.00138	1.35	n.s.					-0.877	0.262	-3.35	< 0.05
Time * Phase	4.10	0.1060	38.8	< 0.05	0.015	0.00425	3.53	< 0.05	-0.0145	0.00446	-3.25	< 0.05	-0.418	0.283	-1.48	n.s.

Table S3. Model selection using the second-order Akaike information criterion (AICc) to compare fits of linear models of spatially-standardised non-flying terrestrial species richness (SQS, quorum = 0.6; GCR quota = 5 occupied grid cells/1000 km MST length) as a function of time and diversification phase.

model	df	logLik	AICc	delta AICc	weights	cumulative weights	evidence ratio
1000 km summed MST distance							
Time * Phase	4	-69.7	150.0	0.00	8.76e-01	0.876	1.00
Phase Only	2	-74.3	155.0	4.82	7.88e-02	0.955	11.10
Time + Phase	3	-73.8	156.0	5.97	4.44e-02	0.999	19.70
Time Only	2	-79.0	164.0	14.20	7.08e-04	1.000	1240.00
Intercept Only	1	-84.0	172.0	22.10	1.40e-05	1.000	62600.00
1500 km summed MST distance							
Time * Phase	4	-82.4	175.0	0.00	9.49e-01	0.949	1.00
Phase Only	2	-88.0	182.0	6.95	2.94e-02	0.978	32.30
Time + Phase	3	-87.5	183.0	8.00	1.74e-02	0.996	54.50
Time Only	2	-90.3	187.0	11.60	2.89e-03	0.999	328.00
Intercept Only	1	-92.2	188.0	13.30	1.24e-03	1.000	765.00
2000 km summed MST distance							
Time * Phase	4	-79.8	170.0	0.00	9.67e-01	0.967	1.00

model	df	logLik	AICc	delta AICc	weights	cumulative weights	evidence ratio
Time + Phase	3	-85.0	178.0	8.17	1.63e-02	0.983	59.30
Phase Only	2	-86.4	179.0	8.86	1.15e-02	0.995	84.10
Intercept Only	1	-88.7	181.0	11.30	3.41e-03	0.998	284.00
Time Only	2	-88.3	183.0	12.60	1.78e-03	1.000	543.00
2500 km summed MST distance							
Time * Phase	4	-56.2	123.0	0.00	9.98e-01	0.998	1.00
Phase Only	2	-65.5	137.0	14.20	8.16e-04	0.999	1220.00
Time + Phase	3	-64.6	137.0	14.50	7.00e-04	1.000	1430.00
Intercept Only	1	-67.4	139.0	15.90	3.47e-04	1.000	2880.00
Time Only	2	-67.1	140.0	17.30	1.71e-04	1.000	5840.00
3000 km summed MST distance							
Time * Phase	4	-42.3	95.3	0.00	9.95e-01	0.995	1.00
Time + Phase	3	-49.3	107.0	11.60	3.03e-03	0.998	328.00
Phase Only	2	-50.9	108.0	12.60	1.81e-03	1.000	550.00
Time Only	2	-54.8	116.0	20.50	3.45e-05	1.000	28800.00
Intercept Only	1	-56.5	117.0	21.80	1.87e-05	1.000	53200.00

model	df	logLik	AICc	delta AICc	weights	cumulative weights	evidence ratio
3500 km summed MST distance							
Time * Phase	4	-35.6	82.0	0.00	9.69e-01	0.969	1.00
Time + Phase	3	-40.8	90.1	8.13	1.67e-02	0.986	58.00
Phase Only	2	-42.2	90.7	8.72	1.24e-02	0.998	78.10
Time Only	2	-45.0	96.2	14.20	7.91e-04	0.999	1230.00
Intercept Only	1	-46.1	96.4	14.40	7.32e-04	1.000	1320.00
4000 km summed MST distance							
Time * Phase	4	-34.2	79.3	0.00	8.46e-01	0.846	1.00
Time + Phase	3	-37.6	83.8	4.47	9.04e-02	0.936	9.36
Phase Only	2	-39.3	84.8	5.47	5.48e-02	0.991	15.40
Intercept Only	1	-42.8	89.7	10.40	4.73e-03	0.996	179.00
Time Only	2	-41.8	89.9	10.60	4.24e-03	1.000	200.00

Table S4. Parameter estimates for coefficients in linear models fitted to spatially-standardised terrestrial tetrapod species richness data (SQS, quorum = 0.6; GCR quota = 5 occupied grid-cells/1000 km MST length). All models fitted to each palaeogeographic spread level are shown, regardless of Akaike weight, and ordering does not reflect importance.

model	Intercept				Time				Time : Phase (Pre-K/Pg)				Phase (Pre-K/Pg)			
	estimate	std.error	statistic	p.value	estimate	std.error	statistic	p.value	estimate	std.error	statistic	p.value	estimate	std.error	statistic	p.value
1000 km summed MST distance																
Intercept Only	3.70	0.0579	64.0	< 0.05												
Phase Only	3.85	0.0615	62.6	< 0.05									-0.546	0.119	-4.58	< 0.05
Time Only	3.83	0.0685	55.9	< 0.05	-0.00224	0.000701	-3.2	< 0.05								
Time + Phase	3.82	0.0653	58.5	< 0.05	0.00123	0.00126	0.977	n.s.					-0.732	0.224	-3.26	< 0.05
Time * Phase	3.69	0.0790	46.7	< 0.05	0.00898	0.00297	3.02	< 0.05	-0.00929	0.00326	-2.85	< 0.05	-0.335	0.257	-1.3	n.s.
1500 km summed MST distance																
Intercept Only	3.80	0.0703	54.1	< 0.05												
Phase Only	3.89	0.0748	52.0	< 0.05									-0.509	0.173	-2.94	< 0.05
Time Only	3.88	0.0818	47.5	< 0.05	-0.00185	0.000952	-1.94	n.s.								
Time + Phase	3.86	0.0802	48.2	< 0.05	0.00186	0.00181	1.03	n.s.					-0.807	0.337	-2.39	< 0.05
Time * Phase	3.68	0.0959	38.4	< 0.05	0.0136	0.00403	3.37	< 0.05	-0.0143	0.00446	-3.21	< 0.05	-0.161	0.379	-0.425	n.s.
2000 km summed MST distance																
Intercept Only	3.87	0.0825	47.0	< 0.05												

model	Intercept				Time				Time : Phase (Pre-K/Pg)				Phase (Pre-K/Pg)			
	estimate	std.error	statistic	p.value	estimate	std.error	statistic	p.value	estimate	std.error	statistic	p.value	estimate	std.error	statistic	p.value
Phase Only	3.98	0.0948	42.0	< 0.05									-0.386	0.181	-2.13	< 0.05
Time Only	3.93	0.1020	38.5	< 0.05	-0.000934	0.00105	-0.892	n.s.								
Time + Phase	3.93	0.0986	39.8	< 0.05	0.00315	0.00188	1.67	n.s.					-0.856	0.333	-2.57	< 0.05
Time * Phase	3.69	0.1190	30.9	< 0.05	0.0179	0.00489	3.67	< 0.05	-0.017	0.00525	-3.25	< 0.05	-0.241	0.367	-0.658	n.s.
2500 km summed MST distance																
Intercept Only	3.97	0.0666	59.6	< 0.05												
Phase Only	4.04	0.0741	54.5	< 0.05									-0.308	0.158	-1.95	n.s.
Time Only	4.01	0.0800	50.1	< 0.05	-0.00077	0.000936	-0.823	n.s.								
Time + Phase	4.00	0.0780	51.3	< 0.05	0.00215	0.0016	1.35	n.s.					-0.612	0.275	-2.23	< 0.05
Time * Phase	3.77	0.0894	42.2	< 0.05	0.0167	0.00374	4.46	< 0.05	-0.0171	0.00406	-4.21	< 0.05	0.0199	0.29	0.0685	n.s.
3000 km summed MST distance																
Intercept Only	4.02	0.0737	54.5	< 0.05												
Phase Only	4.15	0.0778	53.3	< 0.05									-0.555	0.161	-3.45	< 0.05
Time Only	4.11	0.0873	47.0	< 0.05	-0.00173	0.00095	-1.83	n.s.								
Time + Phase	4.10	0.0807	50.8	< 0.05	0.00286	0.00161	1.78	n.s.					-0.987	0.29	-3.41	< 0.05
Time * Phase	3.89	0.0923	42.1	< 0.05	0.0163	0.00382	4.27	< 0.05	-0.0158	0.00413	-3.81	< 0.05	-0.39	0.305	-1.28	n.s.

model	Intercept				Time				Time : Phase (Pre-K/Pg)				Phase (Pre-K/Pg)			
	estimate	std.error	statistic	p.value	estimate	std.error	statistic	p.value	estimate	std.error	statistic	p.value	estimate	std.error	statistic	p.value
3500 km summed MST distance																
Intercept Only	4.18	0.0695	60.2	< 0.05												
Phase Only	4.28	0.0743	57.6	< 0.05									-0.449	0.158	-2.84	< 0.05
Time Only	4.25	0.0821	51.8	< 0.05	-0.00129	0.000857	-1.51	n.s.								
Time + Phase	4.24	0.0772	54.9	< 0.05	0.00257	0.00155	1.66	n.s.					-0.873	0.3	-2.91	< 0.05
Time * Phase	4.07	0.0883	46.1	< 0.05	0.0132	0.00357	3.71	< 0.05	-0.0127	0.0039	-3.26	< 0.05	-0.333	0.323	-1.03	n.s.
4000 km summed MST distance																
Intercept Only	4.17	0.0792	52.7	< 0.05												
Phase Only	4.30	0.0876	49.0	< 0.05									-0.451	0.167	-2.7	< 0.05
Time Only	4.25	0.0959	44.3	< 0.05	-0.00124	0.000899	-1.38	n.s.								
Time + Phase	4.25	0.0893	47.7	< 0.05	0.00296	0.00166	1.78	n.s.					-0.951	0.325	-2.93	< 0.05
Time * Phase	4.09	0.1060	38.4	< 0.05	0.0142	0.00462	3.08	< 0.05	-0.0128	0.00491	-2.6	< 0.05	-0.513	0.35	-1.46	n.s.

Table S5. Model selection using the second-order Akaike information criterion (AICc) to compare fits of linear models of spatially-standardised non-flying terrestrial species richness (face-value species counts) as a function of time and diversification phase.

model	df	logLik	AICc	delta AICc	weights	cumulative weights	evidence ratio
1000 km summed MST distance							
Time * Phase	4	-76.2	163	0.00	8.20e-01	0.820	1.00e+00
Phase Only	2	-80.2	166	3.65	1.32e-01	0.952	6.21e+00
Time + Phase	3	-80.2	169	5.77	4.57e-02	0.998	1.79e+01
Time Only	2	-84.1	174	11.60	2.52e-03	1.000	3.25e+02
Intercept Only	1	-93.0	190	27.20	1.00e-06	1.000	8.12e+05
1500 km summed MST distance							
Time * Phase	4	-78.9	168	0.00	9.81e-01	0.981	1.00e+00
Phase Only	2	-85.4	177	8.69	1.28e-02	0.994	7.66e+01
Time + Phase	3	-85.2	179	10.50	5.20e-03	0.999	1.89e+02
Time Only	2	-88.4	183	14.80	5.90e-04	1.000	1.66e+03
Intercept Only	1	-92.5	189	20.80	2.99e-05	1.000	3.28e+04
2000 km summed MST distance							
Time * Phase	4	-79.5	169	0.00	8.34e-01	0.834	1.00e+00

model	df	logLik	AICc	delta AICc	weights	cumulative weights	evidence ratio
Phase Only	2	-83.7	174	4.23	1.00e-01	0.934	8.34e+00
Time + Phase	3	-83.2	175	5.22	6.15e-02	0.995	1.36e+01
Time Only	2	-87.1	180	10.90	3.50e-03	0.999	2.38e+02
Intercept Only	1	-89.7	183	14.00	7.49e-04	1.000	1.11e+03
2500 km summed MST distance							
Time * Phase	4	-79.5	169	0.00	9.73e-01	0.973	1.00e+00
Phase Only	2	-85.5	177	7.79	1.98e-02	0.993	4.91e+01
Time + Phase	3	-85.5	179	9.85	7.07e-03	1.000	1.38e+02
Time Only	2	-90.0	186	16.70	2.32e-04	1.000	4.19e+03
Intercept Only	1	-95.9	196	26.50	1.70e-06	1.000	5.66e+05
3000 km summed MST distance							
Time * Phase	4	-70.4	151	0.00	9.77e-01	0.977	1.00e+00
Phase Only	2	-76.7	159	8.12	1.68e-02	0.994	5.82e+01
Time + Phase	3	-76.6	162	10.20	5.88e-03	1.000	1.66e+02
Time Only	2	-80.1	166	14.90	5.54e-04	1.000	1.76e+03
Intercept Only	1	-85.9	176	24.60	4.40e-06	1.000	2.20e+05

model	df	logLik	AICc	delta AICc	weights	cumulative weights	evidence ratio
3500 km summed MST distance							
Time * Phase	4	-68.5	147	0.00	9.56e-01	0.956	1.00e+00
Phase Only	2	-74.1	154	6.91	3.02e-02	0.986	3.17e+01
Time + Phase	3	-73.8	156	8.45	1.40e-02	1.000	6.83e+01
Time Only	2	-80.3	167	19.20	6.41e-05	1.000	1.49e+04
Intercept Only	1	-86.9	178	30.40	2.00e-07	1.000	4.00e+06
4000 km summed MST distance							
Time * Phase	4	-68.1	147	0.00	8.84e-01	0.884	1.00e+00
Phase Only	2	-72.6	151	4.74	8.28e-02	0.967	1.07e+01
Time + Phase	3	-72.5	153	6.65	3.18e-02	0.999	2.78e+01
Time Only	2	-76.8	160	13.10	1.26e-03	1.000	7.02e+02
Intercept Only	1	-82.1	168	21.50	1.89e-05	1.000	4.68e+04

Table S6. Parameter estimates for coefficients in linear models fitted to spatially-standardised terrestrial tetrapod species richness data (face-value species counts). All models fitted to each palaeogeographic spread level are shown, regardless of Akaike weight, and ordering does not reflect importance.

model	Intercept				Time				Time : Phase (Pre-K/Pg)				Phase (Pre-K/Pg)			
	estimate	std.error	statistic	p.value	estimate	std.error	statistic	p.value	estimate	std.error	statistic	p.value	estimate	std.error	statistic	p.value
1000 km summed MST distance																
Intercept Only	4.44	0.0591	75.2	< 0.05												
Phase Only	4.61	0.0607	75.9	< 0.05									-0.645	0.121	-5.34	< 0.05
Time Only	4.62	0.0675	68.4	< 0.05	-0.00307	0.000706	-4.35	< 0.05								
Time + Phase	4.61	0.0654	70.5	< 0.05	-1.59e-05	0.00128	-0.0124	n.s.					-0.643	0.227	-2.83	< 0.05
Time * Phase	4.47	0.0799	55.9	< 0.05	0.00746	0.00293	2.55	< 0.05	-0.0091	0.00323	-2.82	< 0.05	-0.231	0.264	-0.875	n.s.
1500 km summed MST distance																
Intercept Only	4.56	0.0682	66.8	< 0.05												
Phase Only	4.68	0.0712	65.7	< 0.05									-0.61	0.158	-3.87	< 0.05
Time Only	4.68	0.0783	59.8	< 0.05	-0.00261	0.000909	-2.87	< 0.05								
Time + Phase	4.67	0.0762	61.3	< 0.05	0.000948	0.00165	0.575	n.s.					-0.754	0.296	-2.55	< 0.05
Time * Phase	4.47	0.0905	49.3	< 0.05	0.0135	0.00381	3.54	< 0.05	-0.015	0.00417	-3.6	< 0.05	-0.137	0.326	-0.421	n.s.
2000 km summed MST distance																
Intercept Only	4.55	0.0695	65.4	< 0.05												

model	Intercept				Time				Time : Phase (Pre-K/Pg)				Phase (Pre-K/Pg)			
	estimate	std.error	statistic	p.value	estimate	std.error	statistic	p.value	estimate	std.error	statistic	p.value	estimate	std.error	statistic	p.value
Phase Only	4.68	0.0758	61.8	< 0.05									-0.529	0.15	-3.53	< 0.05
Time Only	4.66	0.0842	55.4	< 0.05	-0.00206	0.000901	-2.28	< 0.05								
Time + Phase	4.65	0.0811	57.3	< 0.05	0.00168	0.00158	1.06	n.s.					-0.772	0.274	-2.82	< 0.05
Time * Phase	4.48	0.1000	44.7	< 0.05	0.011	0.00375	2.93	< 0.05	-0.0111	0.0041	-2.72	< 0.05	-0.3	0.316	-0.947	n.s.
2500 km summed MST distance																
Intercept Only	4.51	0.0772	58.4	< 0.05												
Phase Only	4.72	0.0821	57.5	< 0.05									-0.724	0.151	-4.79	< 0.05
Time Only	4.69	0.0892	52.6	< 0.05	-0.00313	0.000888	-3.53	< 0.05								
Time + Phase	4.71	0.0856	55.0	< 0.05	0.000427	0.00145	0.294	n.s.					-0.785	0.26	-3.02	< 0.05
Time * Phase	4.48	0.1040	43.3	< 0.05	0.0151	0.00441	3.43	< 0.05	-0.0163	0.00463	-3.51	< 0.05	-0.305	0.28	-1.09	n.s.
3000 km summed MST distance																
Intercept Only	4.67	0.0830	56.3	< 0.05												
Phase Only	4.88	0.0867	56.2	< 0.05									-0.756	0.167	-4.52	< 0.05
Time Only	4.87	0.0951	51.2	< 0.05	-0.00342	0.000972	-3.52	< 0.05								
Time + Phase	4.87	0.0916	53.2	< 0.05	0.000422	0.00173	0.243	n.s.					-0.82	0.312	-2.63	< 0.05
Time * Phase	4.63	0.1090	42.5	< 0.05	0.0157	0.00456	3.44	< 0.05	-0.0174	0.00487	-3.58	< 0.05	-0.212	0.336	-0.632	n.s.

model	Intercept				Time				Time : Phase (Pre-K/Pg)				Phase (Pre-K/Pg)			
	estimate	std.error	statistic	p.value	estimate	std.error	statistic	p.value	estimate	std.error	statistic	p.value	estimate	std.error	statistic	p.value
3500 km summed MST distance																
Intercept Only	4.72	0.0858	55.0	< 0.05												
Phase Only	4.99	0.0882	56.5	< 0.05									-0.859	0.158	-5.44	< 0.05
Time Only	4.94	0.0989	50.0	< 0.05	-0.00344	0.000915	-3.76	< 0.05								
Time + Phase	4.97	0.0918	54.1	< 0.05	0.00117	0.00151	0.775	n.s.					-1.04	0.283	-3.68	< 0.05
Time * Phase	4.73	0.1110	42.5	< 0.05	0.0154	0.00454	3.39	< 0.05	-0.0157	0.00478	-3.3	< 0.05	-0.543	0.306	-1.78	n.s.
4000 km summed MST distance																
Intercept Only	4.75	0.0941	50.5	< 0.05												
Phase Only	5.01	0.1000	50.1	< 0.05									-0.819	0.178	-4.59	< 0.05
Time Only	4.97	0.1100	45.1	< 0.05	-0.00331	0.000997	-3.32	< 0.05								
Time + Phase	5.00	0.1050	47.7	< 0.05	0.000864	0.00169	0.51	n.s.					-0.955	0.322	-2.97	< 0.05
Time * Phase	4.74	0.1310	36.2	< 0.05	0.0159	0.00527	3.01	< 0.05	-0.0166	0.00553	-2.99	< 0.05	-0.431	0.351	-1.23	n.s.

Table S7. Model selection using the second-order Akaike information criterion (AICc) to compare fits of linear models of spatially-standardised non-flying terrestrial species richness (squares extrapolated species richness) as a function of time and diversification phase.

model	df	logLik	AICc	delta AICc	weights	cumulative weights	evidence ratio
1000 km summed MST distance							
Time * Phase	4	-74.3	159	0.00	9.73e-01	0.973	1.00e+00
Phase Only	2	-80.6	167	8.43	1.44e-02	0.987	6.76e+01
Time + Phase	3	-79.7	168	8.75	1.22e-02	1.000	7.98e+01
Time Only	2	-85.1	176	17.40	1.65e-04	1.000	5.90e+03
Intercept Only	1	-88.5	181	22.20	1.50e-05	1.000	6.49e+04
1500 km summed MST distance							
Time * Phase	4	-77.1	165	0.00	9.82e-01	0.982	1.00e+00
Phase Only	2	-84.0	174	9.35	9.16e-03	0.991	1.07e+02
Time + Phase	3	-83.1	174	9.67	7.81e-03	0.999	1.26e+02
Time Only	2	-86.9	180	15.30	4.76e-04	0.999	2.06e+03
Intercept Only	1	-88.6	181	16.60	2.41e-04	1.000	4.07e+03
2000 km summed MST distance							
Time * Phase	4	-76.8	164	0.00	8.65e-01	0.865	1.00e+00

model	df	logLik	AICc	delta AICc	weights	cumulative weights	evidence ratio
Time + Phase	3	-80.3	169	4.88	7.54e-02	0.940	1.15e+01
Phase Only	2	-81.9	170	5.95	4.42e-02	0.985	1.96e+01
Intercept Only	1	-84.4	173	8.85	1.04e-02	0.995	8.32e+01
Time Only	2	-84.0	174	10.10	5.46e-03	1.000	1.58e+02
2500 km summed MST distance							
Time * Phase	4	-75.0	160	0.00	9.95e-01	0.995	1.00e+00
Phase Only	2	-82.9	172	11.50	3.21e-03	0.998	3.10e+02
Time + Phase	3	-82.5	173	12.70	1.70e-03	1.000	5.85e+02
Time Only	2	-87.0	180	19.80	5.09e-05	1.000	1.95e+04
Intercept Only	1	-90.2	184	24.00	6.00e-06	1.000	1.66e+05
3000 km summed MST distance							
Time * Phase	4	-67.1	145	0.00	9.95e-01	0.995	1.00e+00
Phase Only	2	-75.0	156	11.30	3.50e-03	0.998	2.84e+02
Time + Phase	3	-74.8	158	13.10	1.45e-03	1.000	6.86e+02
Time Only	2	-77.5	161	16.30	2.85e-04	1.000	3.49e+03
Intercept Only	1	-80.3	165	19.90	4.66e-05	1.000	2.14e+04

model	df	logLik	AICc	delta AICc	weights	cumulative weights	evidence ratio
3500 km summed MST distance							
Time * Phase	4	-61.8	134	0.00	9.92e-01	0.992	1.00e+00
Time + Phase	3	-68.4	145	11.10	3.87e-03	0.996	2.56e+02
Phase Only	2	-69.5	145	11.10	3.86e-03	1.000	2.57e+02
Time Only	2	-75.2	156	22.40	1.35e-05	1.000	7.35e+04
Intercept Only	1	-78.8	162	27.60	1.00e-06	1.000	1.01e+06
4000 km summed MST distance							
Time * Phase	4	-64.2	139	0.00	9.49e-01	0.949	1.00e+00
Phase Only	2	-69.8	146	6.80	3.17e-02	0.981	2.99e+01
Time + Phase	3	-69.3	147	7.94	1.79e-02	0.999	5.30e+01
Time Only	2	-73.2	152	13.50	1.10e-03	1.000	8.63e+02
Intercept Only	1	-75.7	155	16.50	2.53e-04	1.000	3.75e+03

Table S8. Parameter estimates for coefficients in linear models fitted to spatially-standardised terrestrial tetrapod species richness data (squares extrapolated species richness). All models fitted to each palaeogeographic spread level are shown, regardless of Akaike weight, and ordering does not reflect importance.

model	Intercept				Time				Time : Phase (Pre-K/Pg)				Phase (Pre-K/Pg)			
	estimate	std.error	statistic	p.value	estimate	std.error	statistic	p.value	estimate	std.error	statistic	p.value	estimate	std.error	statistic	p.value
1000 km summed MST distance																
Intercept Only	4.97	0.0566	87.8	< 0.05												
Phase Only	5.09	0.0609	83.6	< 0.05									-0.496	0.121	-4.09	< 0.05
Time Only	5.08	0.0681	74.5	< 0.05	-0.00188	0.000712	-2.64	< 0.05								
Time + Phase	5.06	0.0651	77.8	< 0.05	0.00169	0.00127	1.33	n.s.					-0.75	0.226	-3.31	< 0.05
Time * Phase	4.90	0.0784	62.5	< 0.05	0.0104	0.00287	3.6	< 0.05	-0.0106	0.00317	-3.33	< 0.05	-0.273	0.259	-1.05	n.s.
1500 km summed MST distance																
Intercept Only	5.09	0.0654	77.9	< 0.05												
Phase Only	5.19	0.0701	74.0	< 0.05									-0.482	0.155	-3.1	< 0.05
Time Only	5.17	0.0770	67.2	< 0.05	-0.00166	0.000894	-1.85	n.s.								
Time + Phase	5.16	0.0744	69.3	< 0.05	0.00215	0.00161	1.33	n.s.					-0.807	0.289	-2.79	< 0.05
Time * Phase	4.97	0.0888	55.9	< 0.05	0.014	0.00373	3.75	< 0.05	-0.0142	0.00409	-3.48	< 0.05	-0.223	0.32	-0.696	n.s.
2000 km summed MST distance																
Intercept Only	5.10	0.0655	77.8	< 0.05												

model	Intercept				Time				Time : Phase (Pre-K/Pg)				Phase (Pre-K/Pg)			
	estimate	std.error	statistic	p.value	estimate	std.error	statistic	p.value	estimate	std.error	statistic	p.value	estimate	std.error	statistic	p.value
Phase Only	5.18	0.0743	69.8	< 0.05									-0.329	0.147	-2.24	< 0.05
Time Only	5.14	0.0813	63.2	< 0.05	-0.000777	0.000871	-0.893	n.s.								
Time + Phase	5.13	0.0786	65.3	< 0.05	0.00273	0.00153	1.78	n.s.					-0.724	0.265	-2.73	< 0.05
Time * Phase	4.97	0.0973	51.1	< 0.05	0.0115	0.00364	3.17	< 0.05	-0.0106	0.00398	-2.65	< 0.05	-0.276	0.307	-0.9	n.s.
2500 km summed MST distance																
Intercept Only	5.08	0.0723	70.2	< 0.05												
Phase Only	5.25	0.0797	65.8	< 0.05									-0.579	0.147	-3.95	< 0.05
Time Only	5.21	0.0863	60.3	< 0.05	-0.00218	0.000859	-2.54	< 0.05								
Time + Phase	5.23	0.0827	63.2	< 0.05	0.0013	0.0014	0.923	n.s.					-0.767	0.251	-3.05	< 0.05
Time * Phase	4.98	0.0985	50.6	< 0.05	0.017	0.00419	4.06	< 0.05	-0.0174	0.0044	-3.94	< 0.05	-0.255	0.266	-0.958	n.s.
3000 km summed MST distance																
Intercept Only	5.20	0.0772	67.3	< 0.05												
Phase Only	5.35	0.0849	63.0	< 0.05									-0.548	0.164	-3.35	< 0.05
Time Only	5.33	0.0919	57.9	< 0.05	-0.00226	0.00094	-2.41	< 0.05								
Time + Phase	5.33	0.0894	59.6	< 0.05	0.00105	0.00169	0.618	n.s.					-0.706	0.304	-2.32	< 0.05
Time * Phase	5.07	0.1040	48.5	< 0.05	0.0174	0.00437	3.98	< 0.05	-0.0187	0.00467	-4	< 0.05	-0.0546	0.322	-0.17	n.s.

model	Intercept				Time				Time : Phase (Pre-K/Pg)				Phase (Pre-K/Pg)			
	estimate	std.error	statistic	p.value	estimate	std.error	statistic	p.value	estimate	std.error	statistic	p.value	estimate	std.error	statistic	p.value
3500 km summed MST distance																
Intercept Only	5.27	0.0773	68.3	< 0.05												
Phase Only	5.48	0.0831	66.0	< 0.05									-0.675	0.149	-4.53	< 0.05
Time Only	5.42	0.0926	58.6	< 0.05	-0.00235	0.000857	-2.74	< 0.05								
Time + Phase	5.45	0.0856	63.7	< 0.05	0.00205	0.00141	1.46	n.s.					-0.993	0.264	-3.76	< 0.05
Time * Phase	5.21	0.1020	51.0	< 0.05	0.0167	0.00416	4.02	< 0.05	-0.0163	0.00438	-3.71	< 0.05	-0.479	0.28	-1.71	n.s.
4000 km summed MST distance																
Intercept Only	5.33	0.0859	62.1	< 0.05												
Phase Only	5.52	0.0960	57.5	< 0.05									-0.605	0.171	-3.53	< 0.05
Time Only	5.48	0.1050	52.4	< 0.05	-0.00214	0.000946	-2.26	< 0.05								
Time + Phase	5.50	0.0999	55.0	< 0.05	0.00163	0.00162	1.01	n.s.					-0.861	0.307	-2.8	< 0.05
Time * Phase	5.23	0.1240	42.2	< 0.05	0.0169	0.00499	3.39	< 0.05	-0.0168	0.00523	-3.22	< 0.05	-0.328	0.332	-0.988	n.s.

Table S9. Model selection using the second-order Akaike information criterion (AICc) to compare fits of linear models of spatially-standardised non-flying terrestrial species richness (Chao 2 extrapolated species richness) as a function of time and diversification phase.

model	df	logLik	AICc	delta AICc	weights	cumulative weights	evidence ratio
1000 km summed MST distance							
Time * Phase	4	-71.9	154	0.00	8.40e-01	0.840	1.00e+00
Phase Only	2	-76.2	159	4.44	9.14e-02	0.931	9.19e+00
Time + Phase	3	-75.5	159	5.07	6.64e-02	0.998	1.27e+01
Time Only	2	-80.1	166	12.30	1.82e-03	1.000	4.62e+02
Intercept Only	1	-83.3	171	16.40	2.27e-04	1.000	3.70e+03
1500 km summed MST distance							
Time * Phase	4	-72.1	155	0.00	9.91e-01	0.991	1.00e+00
Time + Phase	3	-78.7	166	10.90	4.21e-03	0.995	2.35e+02
Phase Only	2	-79.8	166	11.00	4.07e-03	0.999	2.43e+02
Time Only	2	-82.4	171	16.10	3.10e-04	1.000	3.20e+03
Intercept Only	1	-83.5	171	16.30	2.84e-04	1.000	3.49e+03
2000 km summed MST distance							
Time * Phase	4	-71.2	153	0.00	9.43e-01	0.943	1.00e+00

model	df	logLik	AICc	delta AICc	weights	cumulative weights	evidence ratio
Time + Phase	3	-75.8	160	7.05	2.77e-02	0.971	3.40e+01
Phase Only	2	-77.4	161	8.13	1.62e-02	0.987	5.82e+01
Intercept Only	1	-79.0	162	9.23	9.36e-03	0.996	1.01e+02
Time Only	2	-78.9	164	11.00	3.78e-03	1.000	2.49e+02
2500 km summed MST distance							
Time * Phase	4	-67.5	146	0.00	9.99e-01	0.999	1.00e+00
Time + Phase	3	-76.2	161	15.00	5.45e-04	1.000	1.83e+03
Phase Only	2	-77.3	161	15.10	5.23e-04	1.000	1.91e+03
Time Only	2	-81.3	169	23.30	8.90e-06	1.000	1.12e+05
Intercept Only	1	-83.1	170	24.80	4.20e-06	1.000	2.39e+05
3000 km summed MST distance							
Time * Phase	4	-64.4	139	0.00	9.88e-01	0.988	1.00e+00
Phase Only	2	-71.6	149	9.97	6.76e-03	0.995	1.46e+02
Time + Phase	3	-70.9	150	10.80	4.41e-03	0.999	2.24e+02
Time Only	2	-74.6	155	16.00	3.29e-04	0.999	3.00e+03
Intercept Only	1	-76.8	158	18.20	1.11e-04	1.000	8.90e+03

model	df	logLik	AICc	delta AICc	weights	cumulative weights	evidence ratio
3500 km summed MST distance							
Time * Phase	4	-53.3	117	0.00	9.94e-01	0.994	1.00e+00
Time + Phase	3	-60.3	129	11.60	2.96e-03	0.997	3.36e+02
Phase Only	2	-61.5	129	11.90	2.59e-03	1.000	3.84e+02
Time Only	2	-67.3	141	23.50	7.70e-06	1.000	1.29e+05
Intercept Only	1	-70.9	146	28.60	6.00e-07	1.000	1.62e+06
4000 km summed MST distance							
Time * Phase	4	-57.8	126	0.00	9.43e-01	0.943	1.00e+00
Phase Only	2	-63.4	133	6.79	3.17e-02	0.975	2.97e+01
Time + Phase	3	-62.6	134	7.33	2.42e-02	0.999	3.90e+01
Time Only	2	-67.0	140	14.00	8.71e-04	1.000	1.08e+03
Intercept Only	1	-69.2	142	16.20	2.87e-04	1.000	3.29e+03

Table S10. Parameter estimates for coefficients in linear models fitted to spatially-standardised terrestrial tetrapod species richness data (Chao 2 extrapolated species richness). All models fitted to each palaeogeographic spread level are shown, regardless of Akaike weight, and ordering does not reflect importance.

model	Intercept				Time				Time : Phase (Pre-K/Pg)				Phase (Pre-K/Pg)			
	estimate	std.error	statistic	p.value	estimate	std.error	statistic	p.value	estimate	std.error	statistic	p.value	estimate	std.error	statistic	p.value
1000 km summed MST distance																
Intercept Only	5.07	0.0538	94.2	< 0.05												
Phase Only	5.18	0.0584	88.7	< 0.05									-0.447	0.116	-3.85	< 0.05
Time Only	5.16	0.0649	79.5	< 0.05	-0.00171	0.000679	-2.51	< 0.05								
Time + Phase	5.15	0.0624	82.5	< 0.05	0.00147	0.00122	1.2	n.s.					-0.668	0.217	-3.08	< 0.05
Time * Phase	5.03	0.0766	65.6	< 0.05	0.00831	0.00281	2.96	< 0.05	-0.00832	0.0031	-2.68	< 0.05	-0.292	0.253	-1.15	n.s.
1500 km summed MST distance																
Intercept Only	5.19	0.0619	83.8	< 0.05												
Phase Only	5.27	0.0671	78.6	< 0.05									-0.408	0.148	-2.75	< 0.05
Time Only	5.25	0.0733	71.6	< 0.05	-0.00128	0.000852	-1.5	n.s.								
Time + Phase	5.23	0.0710	73.7	< 0.05	0.00226	0.00154	1.47	n.s.					-0.75	0.276	-2.72	< 0.05
Time * Phase	5.05	0.0842	59.9	< 0.05	0.0141	0.00354	3.99	< 0.05	-0.0142	0.00388	-3.67	< 0.05	-0.166	0.303	-0.546	n.s.
2000 km summed MST distance																
Intercept Only	5.16	0.0617	83.6	< 0.05												

model	Intercept				Time				Time : Phase (Pre-K/Pg)				Phase (Pre-K/Pg)			
	estimate	std.error	statistic	p.value	estimate	std.error	statistic	p.value	estimate	std.error	statistic	p.value	estimate	std.error	statistic	p.value
Phase Only	5.23	0.0707	73.9	< 0.05									-0.249	0.14	-1.78	n.s.
Time Only	5.19	0.0768	67.5	< 0.05	-0.000429	0.000822	-0.521	n.s.								
Time + Phase	5.18	0.0748	69.3	< 0.05	0.0026	0.00146	1.78	n.s.					-0.625	0.252	-2.48	< 0.05
Time * Phase	5.00	0.0914	54.7	< 0.05	0.0121	0.00342	3.54	< 0.05	-0.0114	0.00374	-3.05	< 0.05	-0.141	0.289	-0.487	n.s.
2500 km summed MST distance																
Intercept Only	5.16	0.0667	77.3	< 0.05												
Phase Only	5.30	0.0748	70.8	< 0.05									-0.482	0.138	-3.51	< 0.05
Time Only	5.25	0.0809	64.8	< 0.05	-0.00153	0.000805	-1.9	n.s.								
Time + Phase	5.27	0.0770	68.4	< 0.05	0.00193	0.00131	1.48	n.s.					-0.762	0.234	-3.26	< 0.05
Time * Phase	5.03	0.0905	55.5	< 0.05	0.0175	0.00385	4.55	< 0.05	-0.0172	0.00405	-4.26	< 0.05	-0.253	0.244	-1.04	n.s.
3000 km summed MST distance																
Intercept Only	5.26	0.0738	71.3	< 0.05												
Phase Only	5.40	0.0813	66.4	< 0.05									-0.514	0.157	-3.28	< 0.05
Time Only	5.36	0.0886	60.5	< 0.05	-0.00188	0.000907	-2.07	< 0.05								
Time + Phase	5.37	0.0851	63.1	< 0.05	0.00182	0.00161	1.13	n.s.					-0.789	0.29	-2.72	< 0.05
Time * Phase	5.14	0.1010	50.9	< 0.05	0.0163	0.00422	3.86	< 0.05	-0.0166	0.00451	-3.67	< 0.05	-0.211	0.311	-0.68	n.s.

model	Intercept				Time				Time : Phase (Pre-K/Pg)				Phase (Pre-K/Pg)			
	estimate	std.error	statistic	p.value	estimate	std.error	statistic	p.value	estimate	std.error	statistic	p.value	estimate	std.error	statistic	p.value
3500 km summed MST distance																
Intercept Only	5.37	0.0697	77.1	< 0.05												
Phase Only	5.56	0.0748	74.3	< 0.05									-0.611	0.134	-4.55	< 0.05
Time Only	5.51	0.0836	65.9	< 0.05	-0.00209	0.000773	-2.71	< 0.05								
Time + Phase	5.53	0.0770	71.8	< 0.05	0.00196	0.00127	1.54	n.s.					-0.914	0.237	-3.85	< 0.05
Time * Phase	5.31	0.0916	58.0	< 0.05	0.0154	0.00373	4.13	< 0.05	-0.0149	0.00393	-3.79	< 0.05	-0.443	0.251	-1.76	n.s.
4000 km summed MST distance																
Intercept Only	5.43	0.0783	69.4	< 0.05												
Phase Only	5.60	0.0877	63.9	< 0.05									-0.546	0.156	-3.49	< 0.05
Time Only	5.55	0.0959	57.9	< 0.05	-0.00181	0.000867	-2.09	< 0.05								
Time + Phase	5.57	0.0909	61.3	< 0.05	0.00186	0.00147	1.26	n.s.					-0.839	0.279	-3	< 0.05
Time * Phase	5.34	0.1130	47.2	< 0.05	0.0154	0.00455	3.37	< 0.05	-0.0149	0.00478	-3.11	< 0.05	-0.368	0.303	-1.21	n.s.

28

720